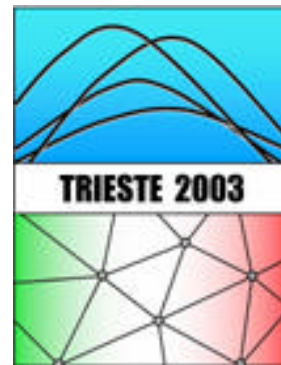


Data-driven imaging with second-order traveltimes approximations

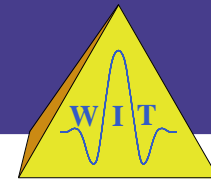
Jürgen Mann

Geophysical Institute
University of Karlsruhe
Germany

EAGE/SEG Summer

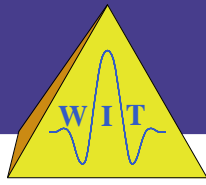
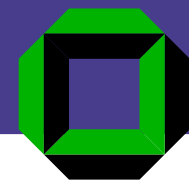


Research Workshop



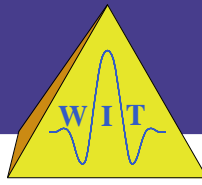
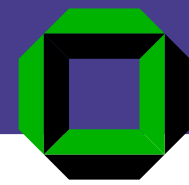
- Motivation & data examples

Overview



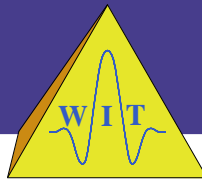
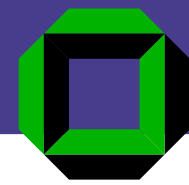
- Motivation & data examples
- Basic concepts

Overview

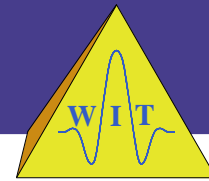


- Motivation & data examples
- Basic concepts
- Possible derivations

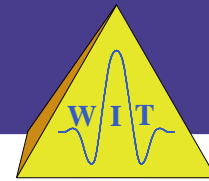
Overview



- Motivation & data examples
- Basic concepts
- Possible derivations
- Hypothetical experiments



- Motivation & data examples
- Basic concepts
- Possible derivations
- Hypothetical experiments
- Applications of wavefield attributes

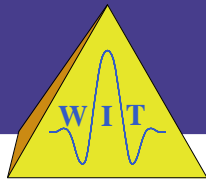
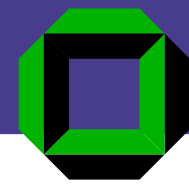


- Motivation & data examples
- Basic concepts
- Possible derivations
- Hypothetical experiments
- Applications of wavefield attributes
- Conclusions



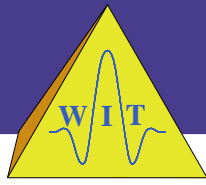
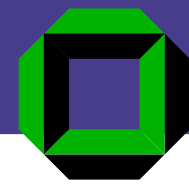
- Motivation & data examples
- Basic concepts
- Possible derivations
- Hypothetical experiments
- Applications of wavefield attributes
- Conclusions
- Outlook

Motivation



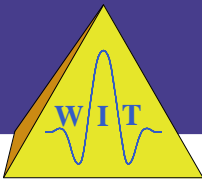
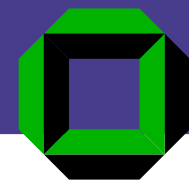
Model-based approaches:

Motivation



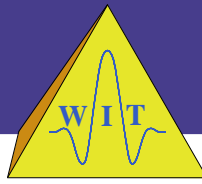
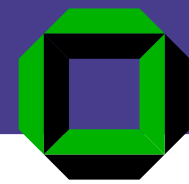
Model-based approaches:

- sensitive to model errors



Model-based approaches:

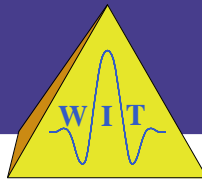
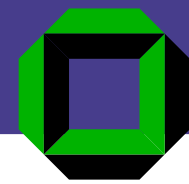
- sensitive to model errors
- migration velocity analysis is costly



Model-based approaches:

- sensitive to model errors
- migration velocity analysis is costly

Data-driven approaches:

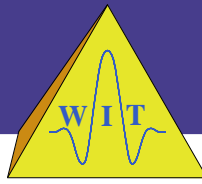
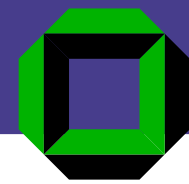


Model-based approaches:

- sensitive to model errors
- migration velocity analysis is costly

Data-driven approaches:

- interval velocity model determination is postponed

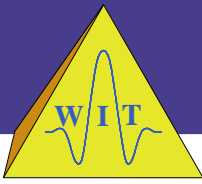
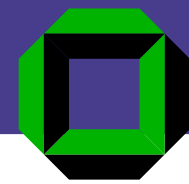


Model-based approaches:

- sensitive to model errors
- migration velocity analysis is costly

Data-driven approaches:

- interval velocity model determination is postponed
- robust methods

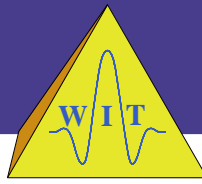
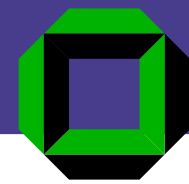


Model-based approaches:

- sensitive to model errors
- migration velocity analysis is costly

Data-driven approaches:

- interval velocity model determination is postponed
- robust methods
- however, classic data-driven approaches

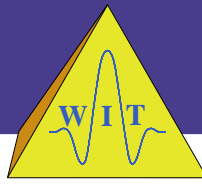
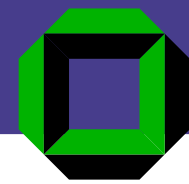


Model-based approaches:

- sensitive to model errors
- migration velocity analysis is costly

Data-driven approaches:

- interval velocity model determination is postponed
- robust methods
- however, classic data-driven approaches
 - use only a subset of available data, thus no optimum S/N ratio

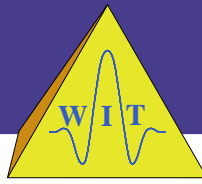
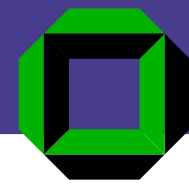


Model-based approaches:

- sensitive to model errors
- migration velocity analysis is costly

Data-driven approaches:

- interval velocity model determination is postponed
- robust methods
- however, classic data-driven approaches
 - use only a subset of available data, thus no optimum S/N ratio
 - provide little information for later inversion

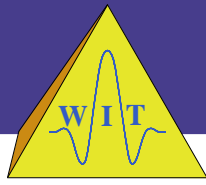
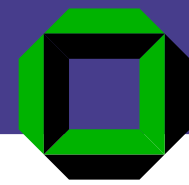


Model-based approaches:

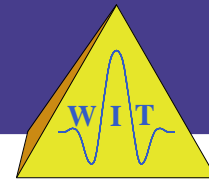
- sensitive to model errors
- migration velocity analysis is costly

Data-driven approaches:

- interval velocity model determination is postponed
- robust methods
- however, classic data-driven approaches
 - use only a subset of available data, thus no optimum S/N ratio
 - provide little information for later inversion
 - data-driven aspects usually not fully exploited

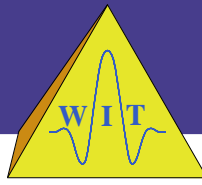
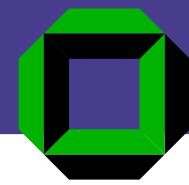


Common-Reflection-Surface (CRS) stack:



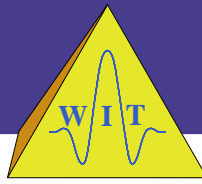
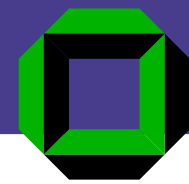
Common-Reflection-Surface (CRS) stack:

- extension of concepts of classic data-driven approaches



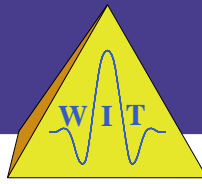
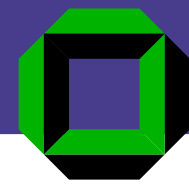
Common-Reflection-Surface (CRS) stack:

- extension of concepts of classic data-driven approaches
- full use of available data



Common-Reflection-Surface (CRS) stack:

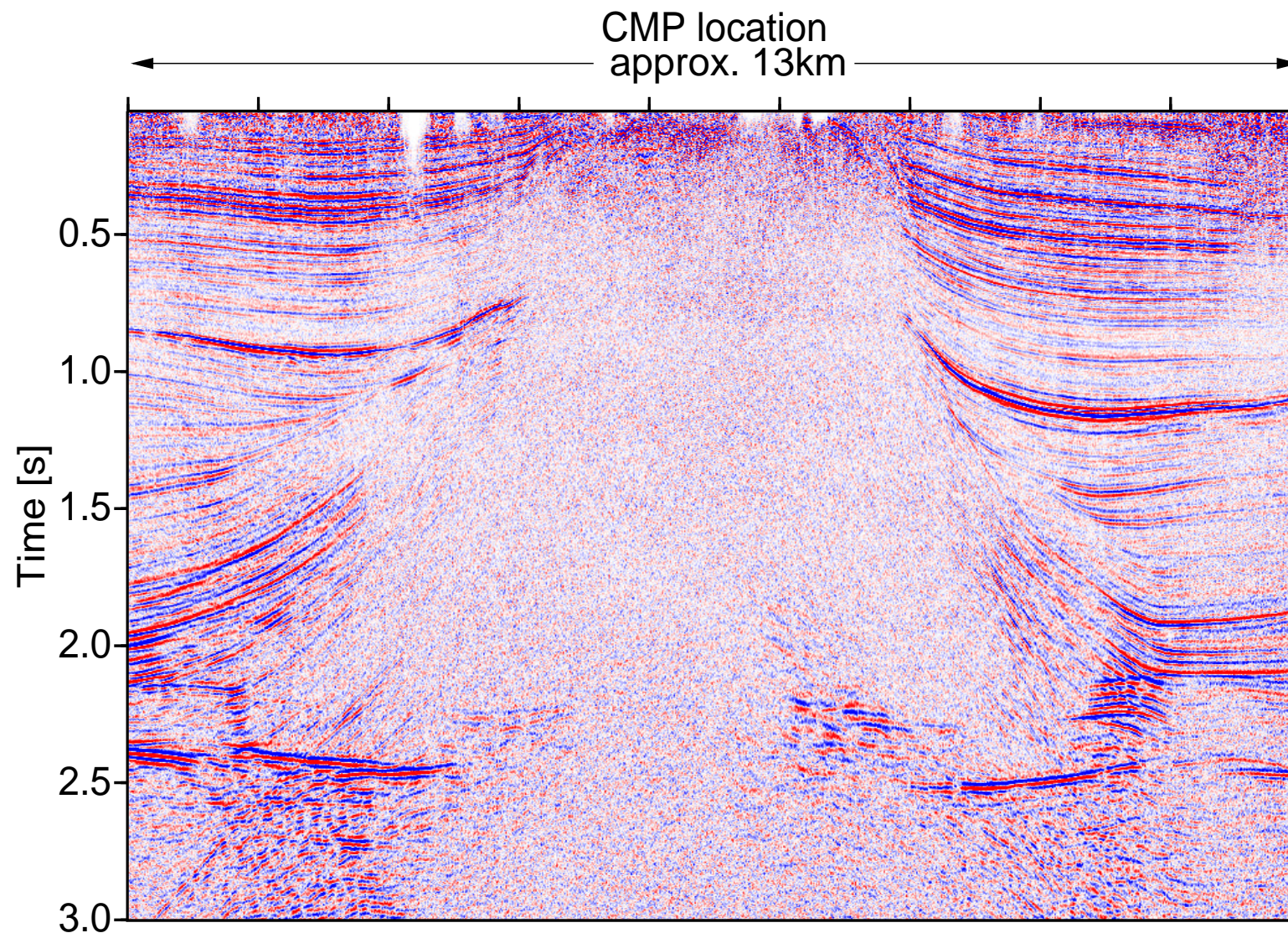
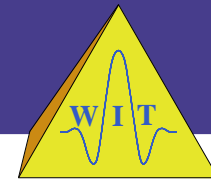
- extension of concepts of classic data-driven approaches
- full use of available data
- minimum a priori information required



Common-Reflection-Surface (CRS) stack:

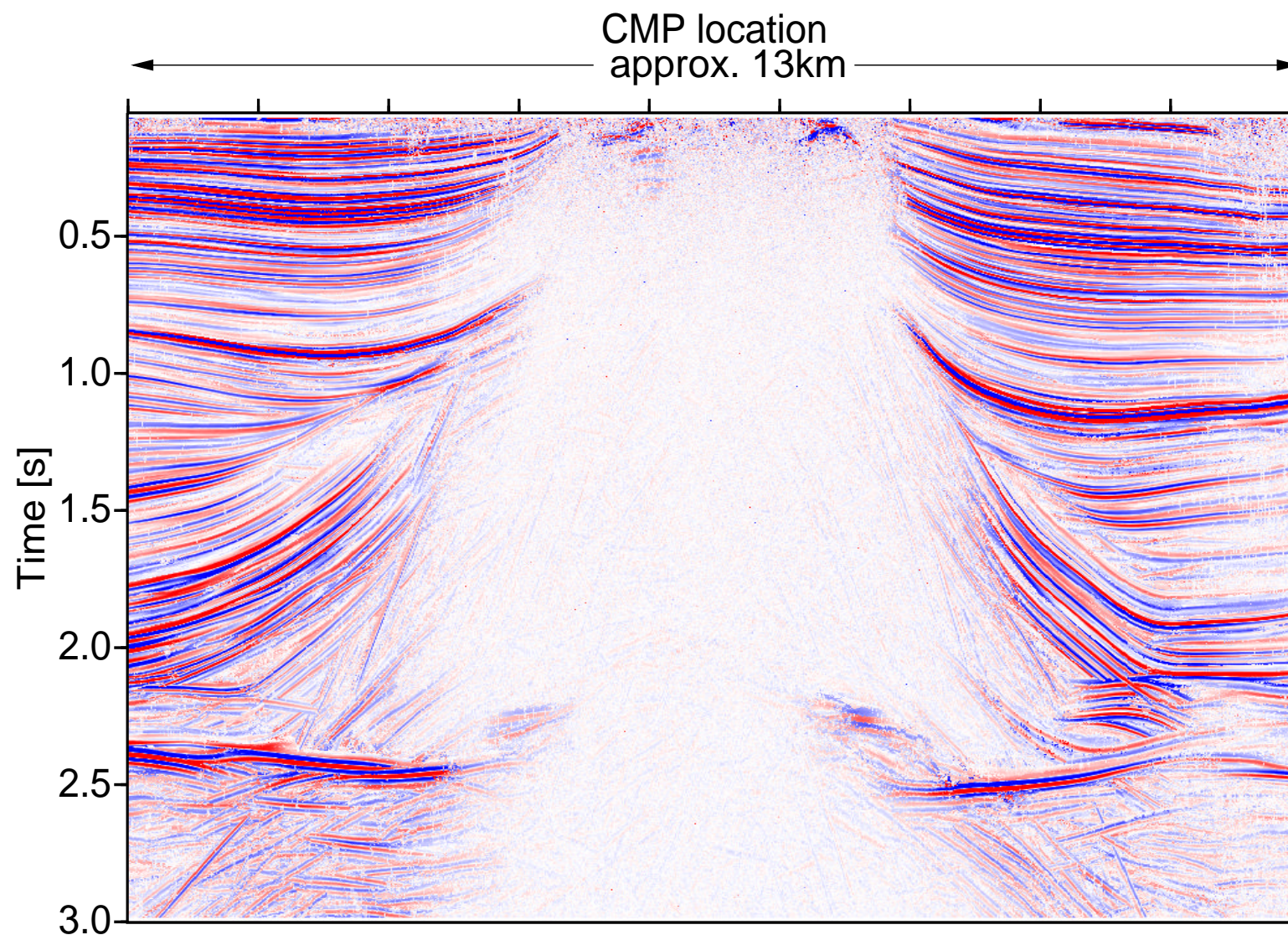
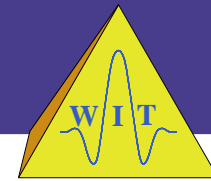
- extension of concepts of classic data-driven approaches
- full use of available data
- minimum a priori information required
- fully data-driven application

Data example A



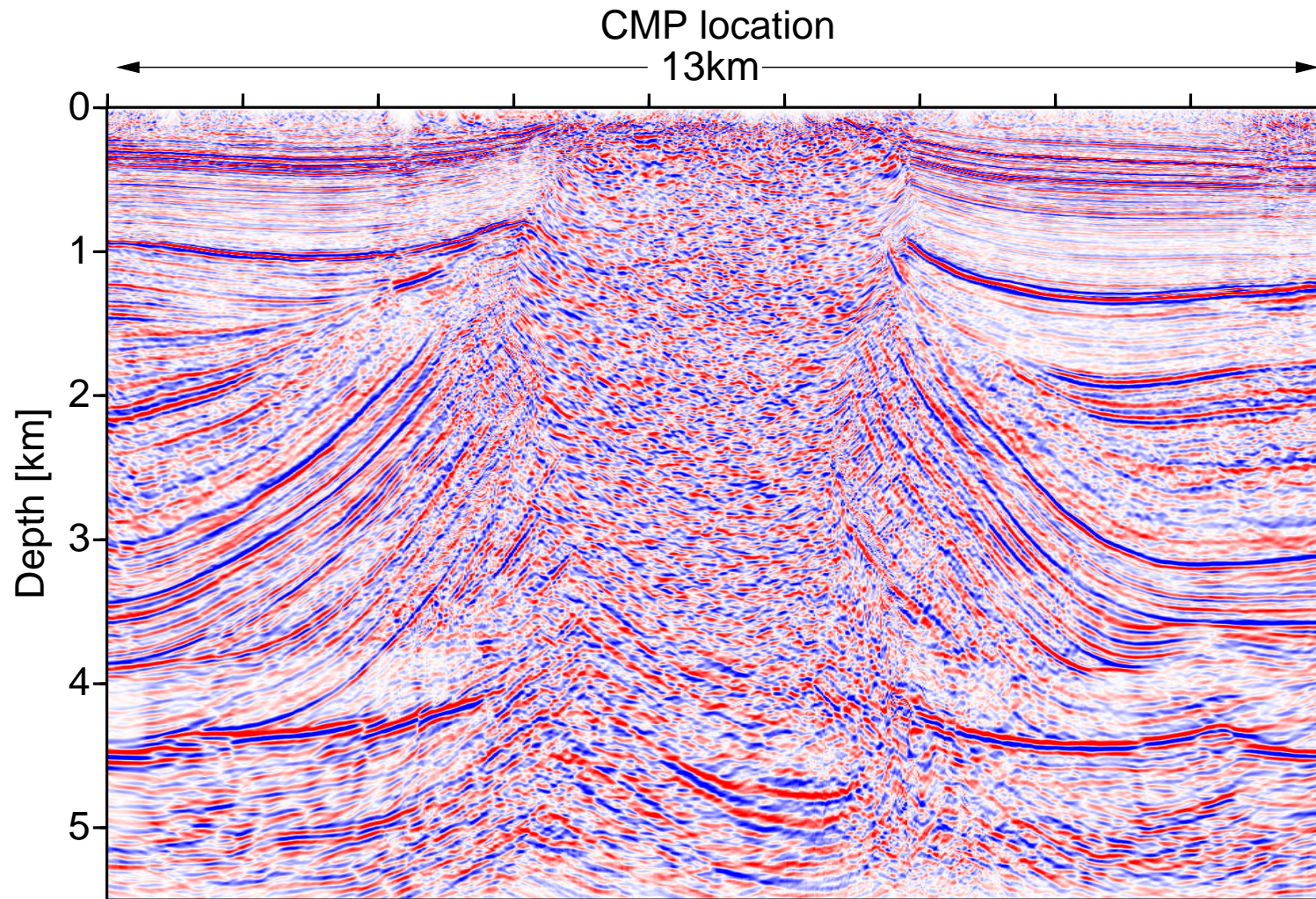
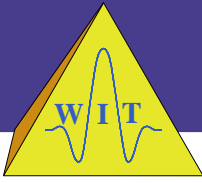
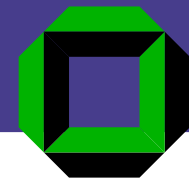
2-D NMO/DMO/stack – from Müller (1999)

Data example A



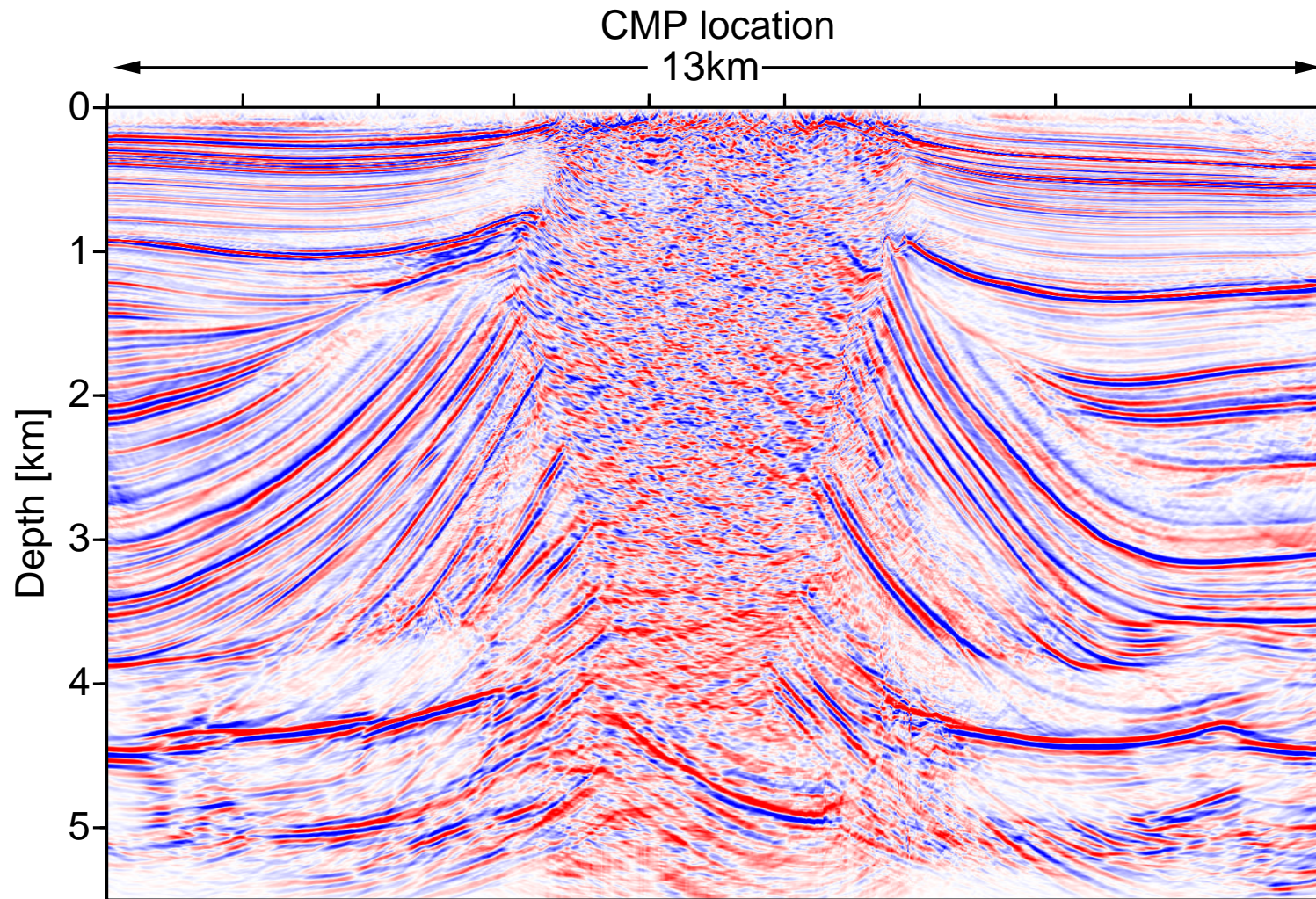
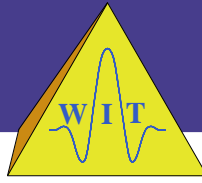
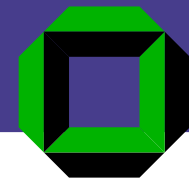
2-D CRS stack – from Müller (1999)

Data example A



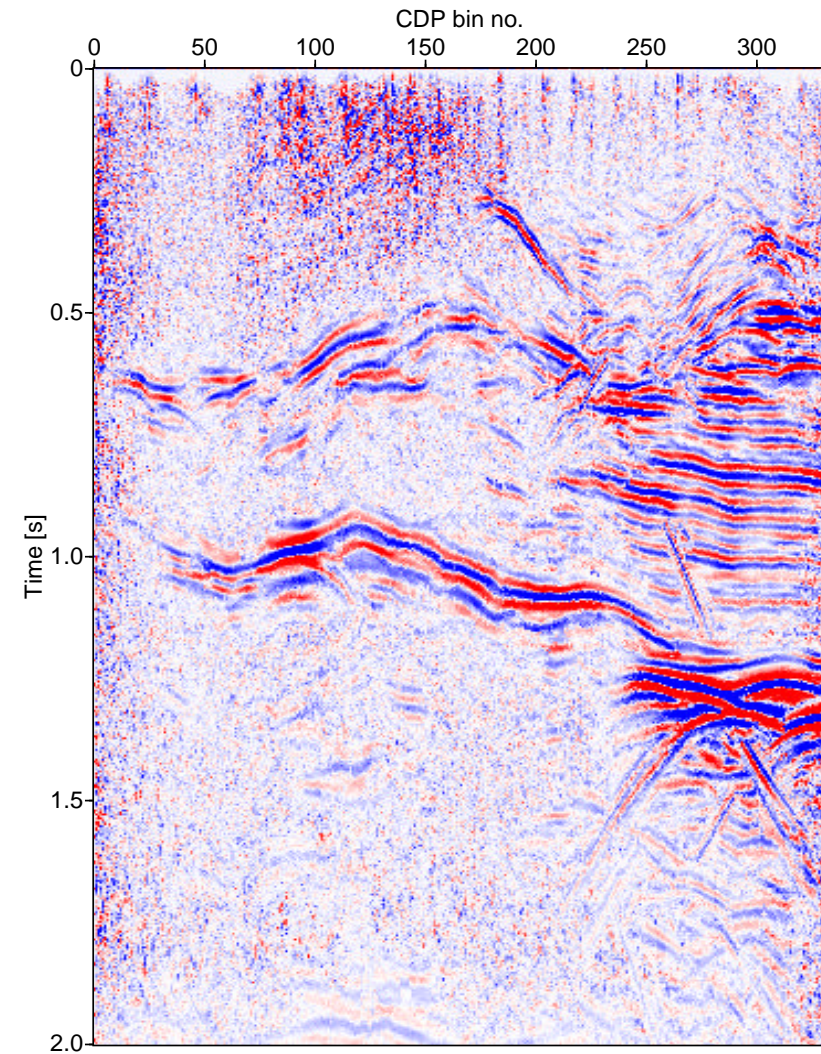
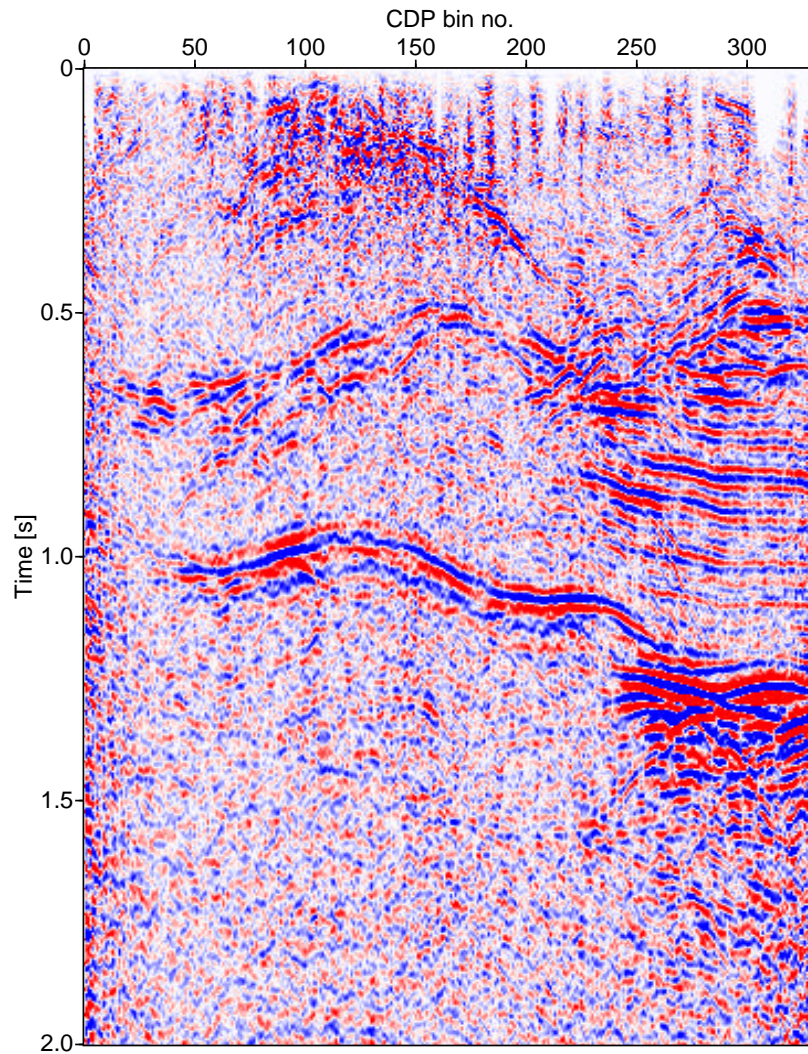
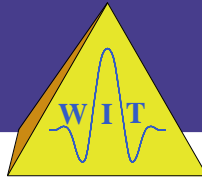
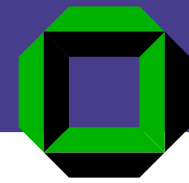
NMO/DMO/stack/poststack migration – from Müller (1999)

Data example A



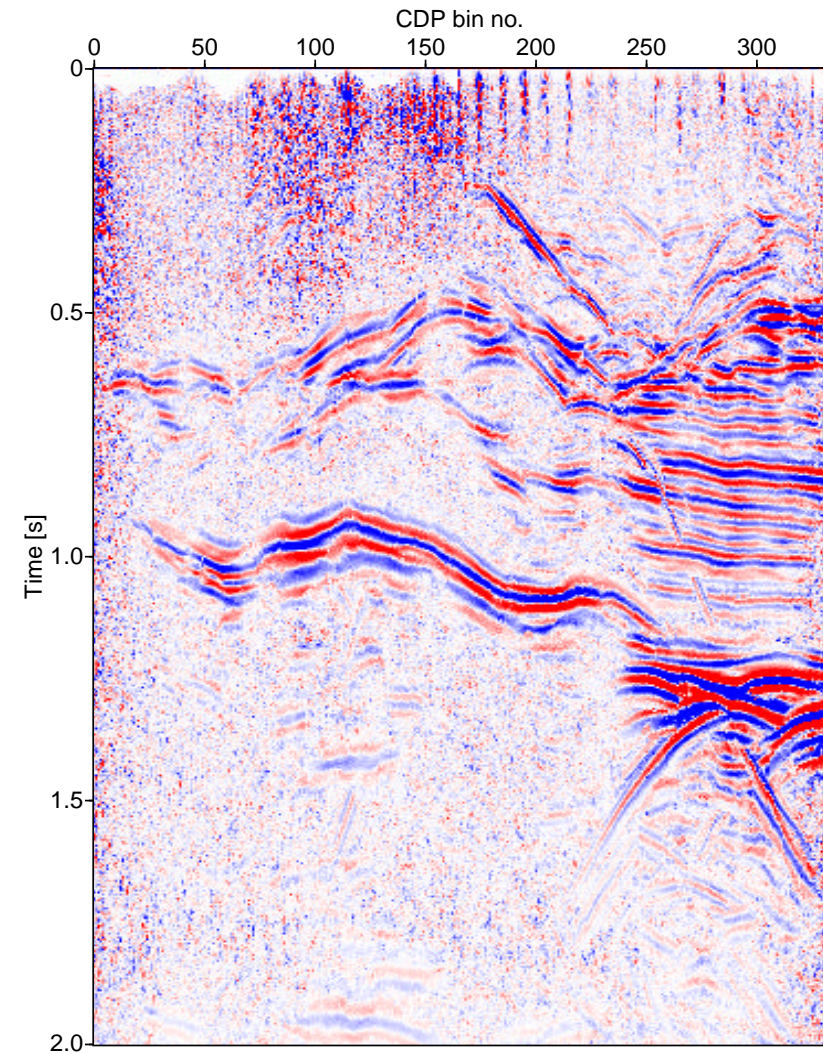
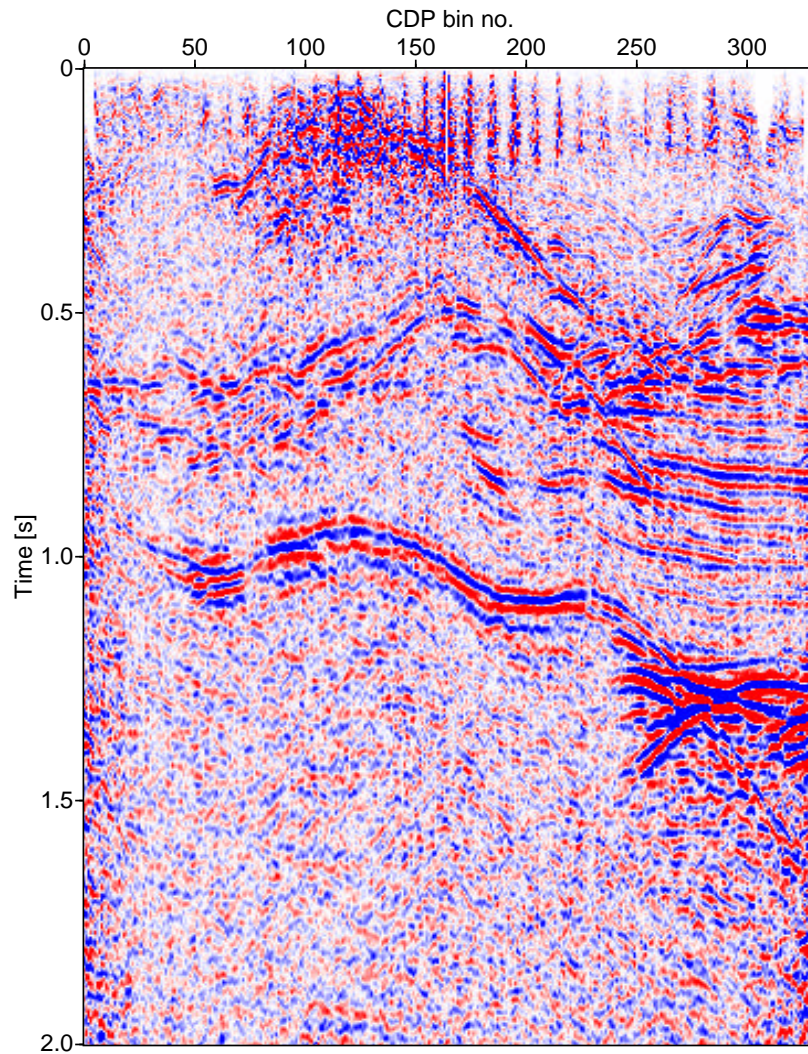
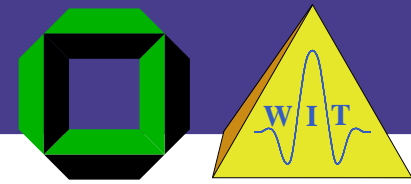
2-D CRS/poststack migration – from Müller (1999)

Data example B



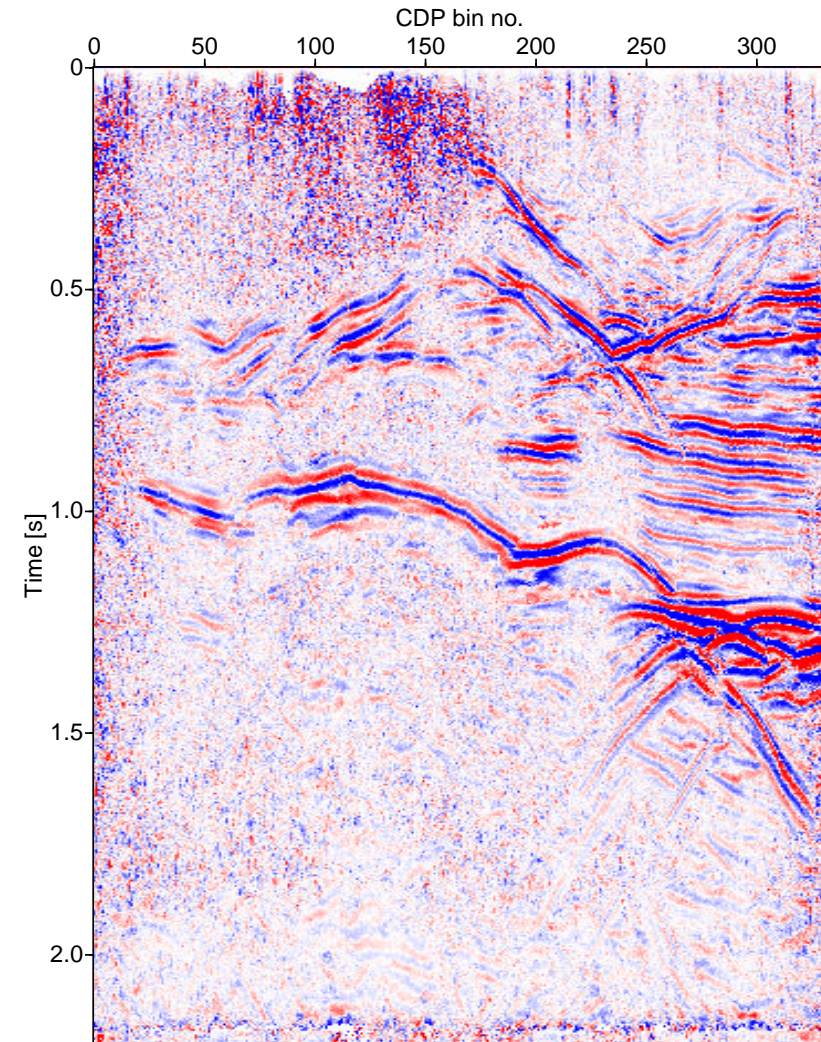
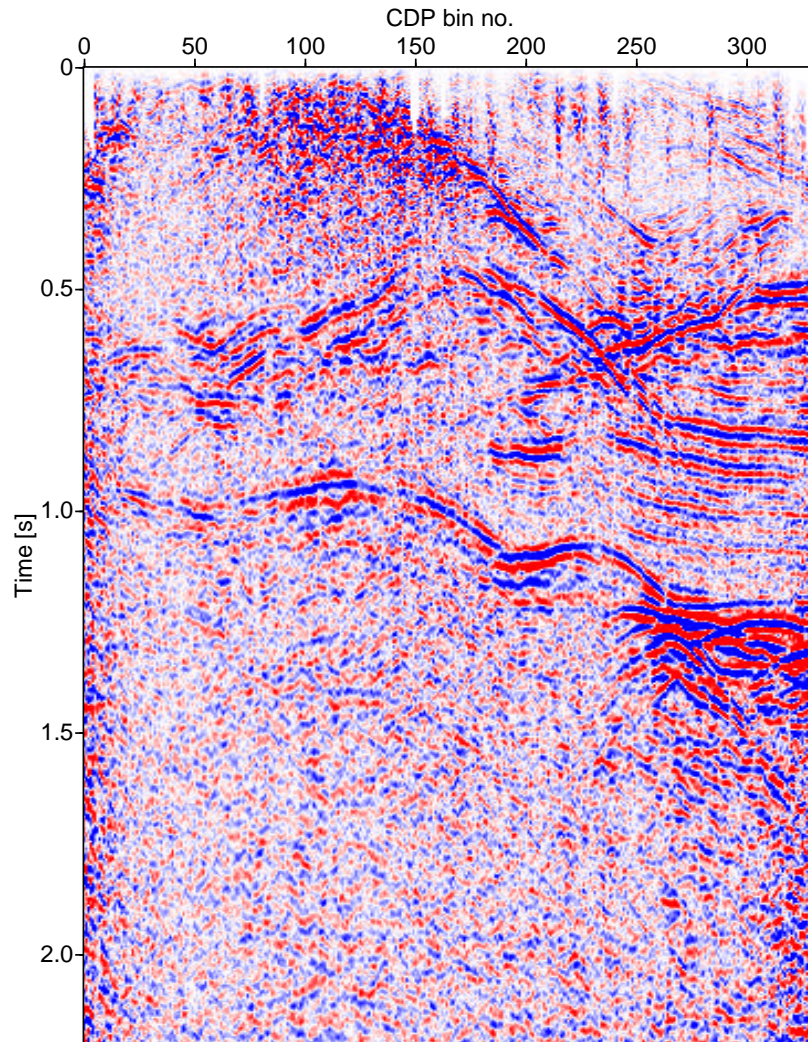
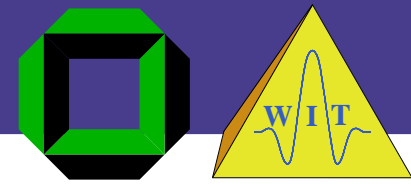
NMO/DMO/stack vs. CRS stack – 3-D data, inline A
From Bergler et. al (2002). Data courtesy of ENI E & P Division.

Data example B



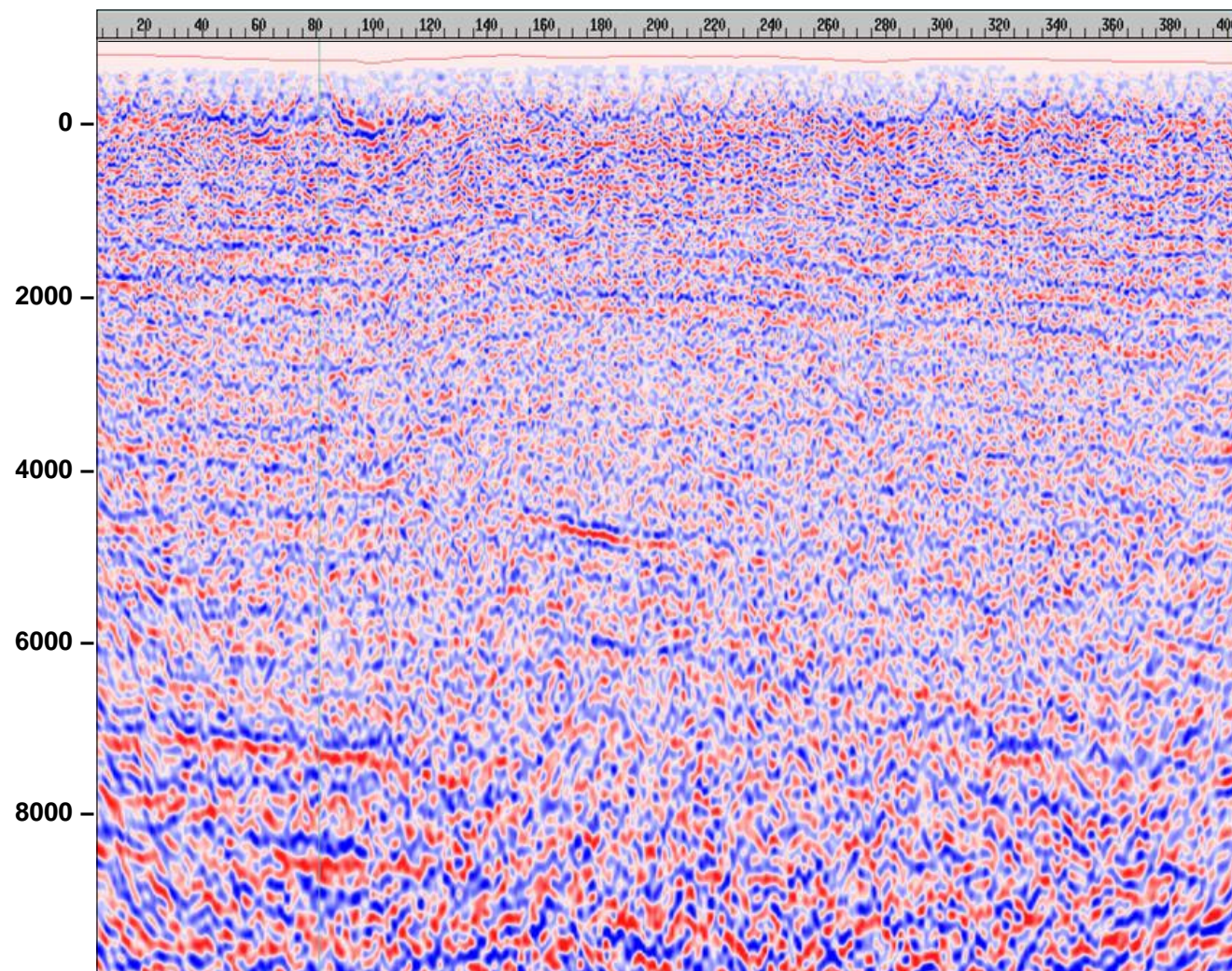
NMO/DMO/stack vs. CRS stack – 3-D data, inline B
From Bergler et. al (2002). Data courtesy of ENI E & P Division.

Data example B



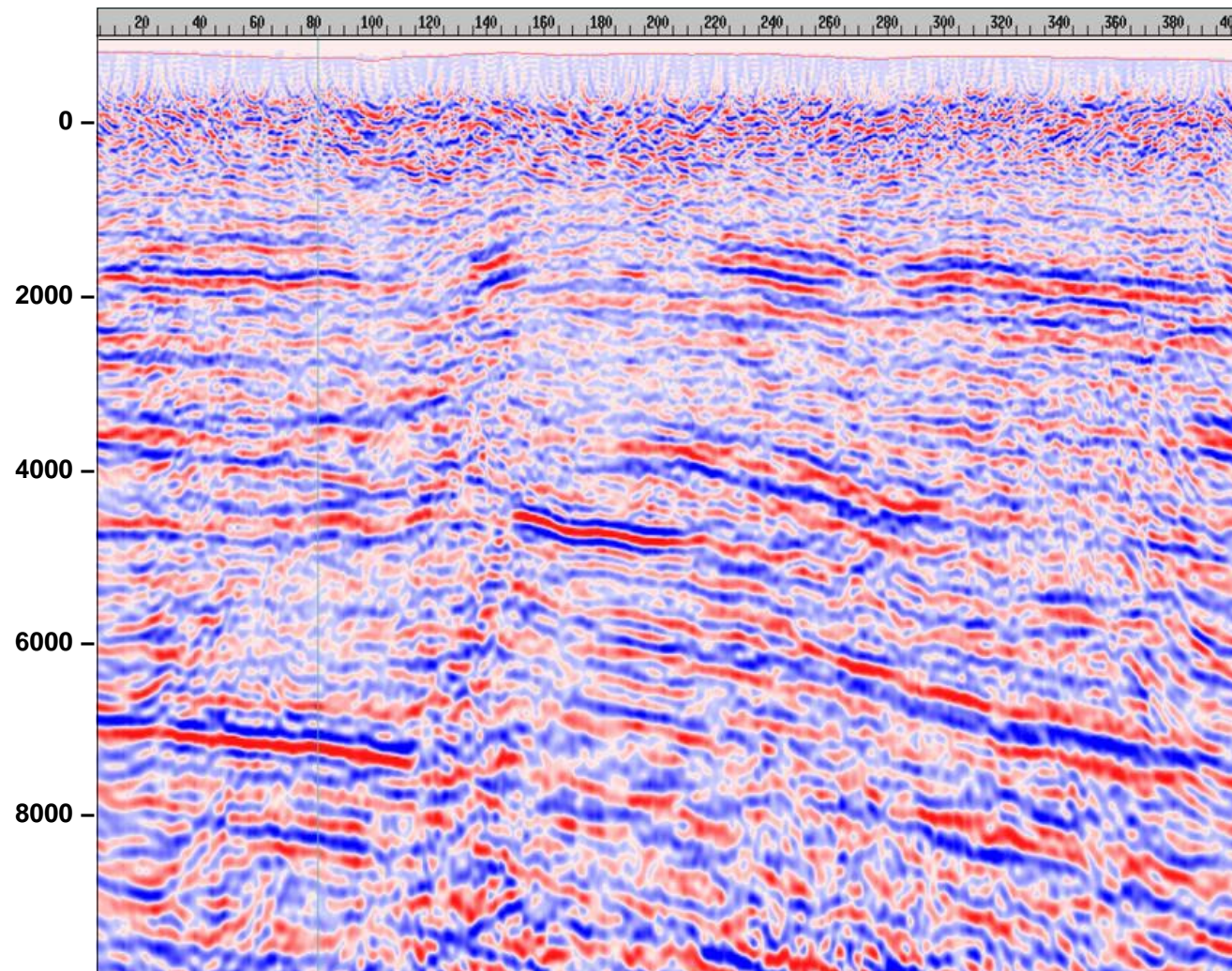
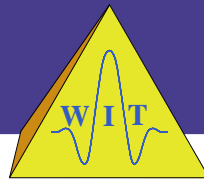
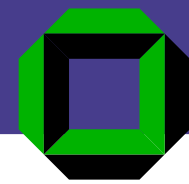
NMO/DMO/stack vs. CRS stack – 3-D data, inline C
From Bergler et. al (2002). Data courtesy of ENI E & P Division.

Data example C



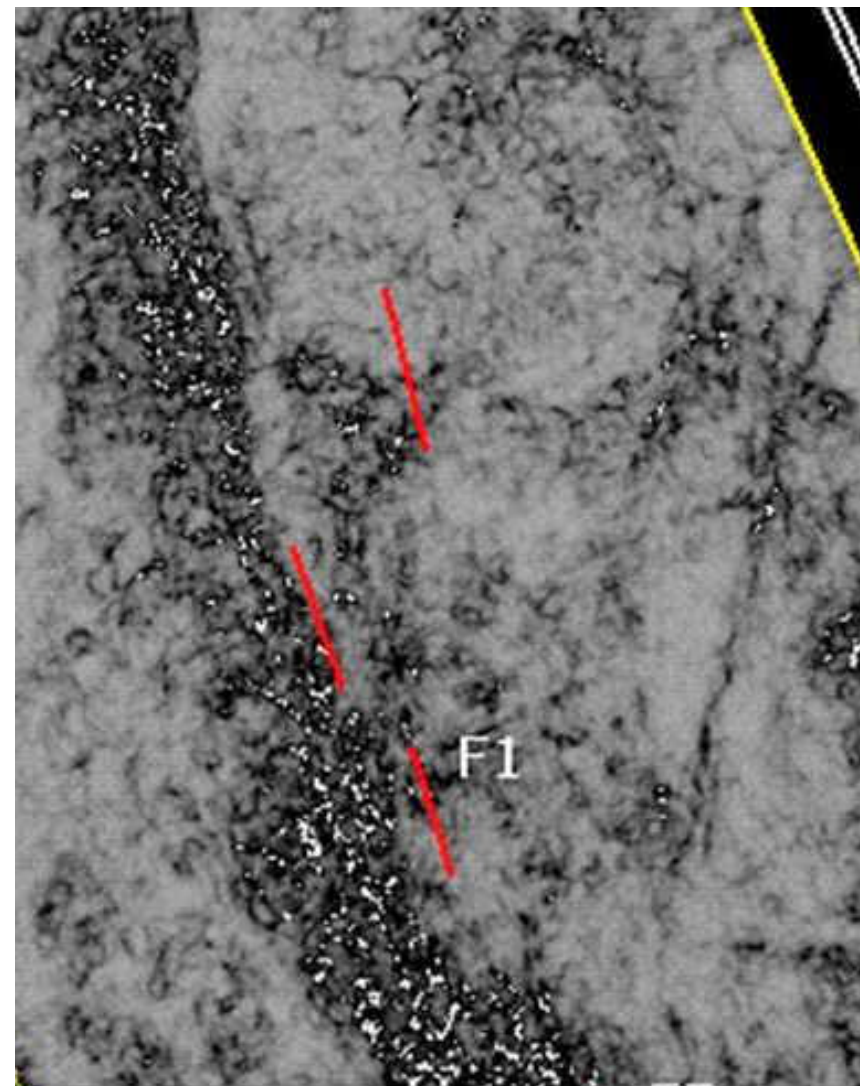
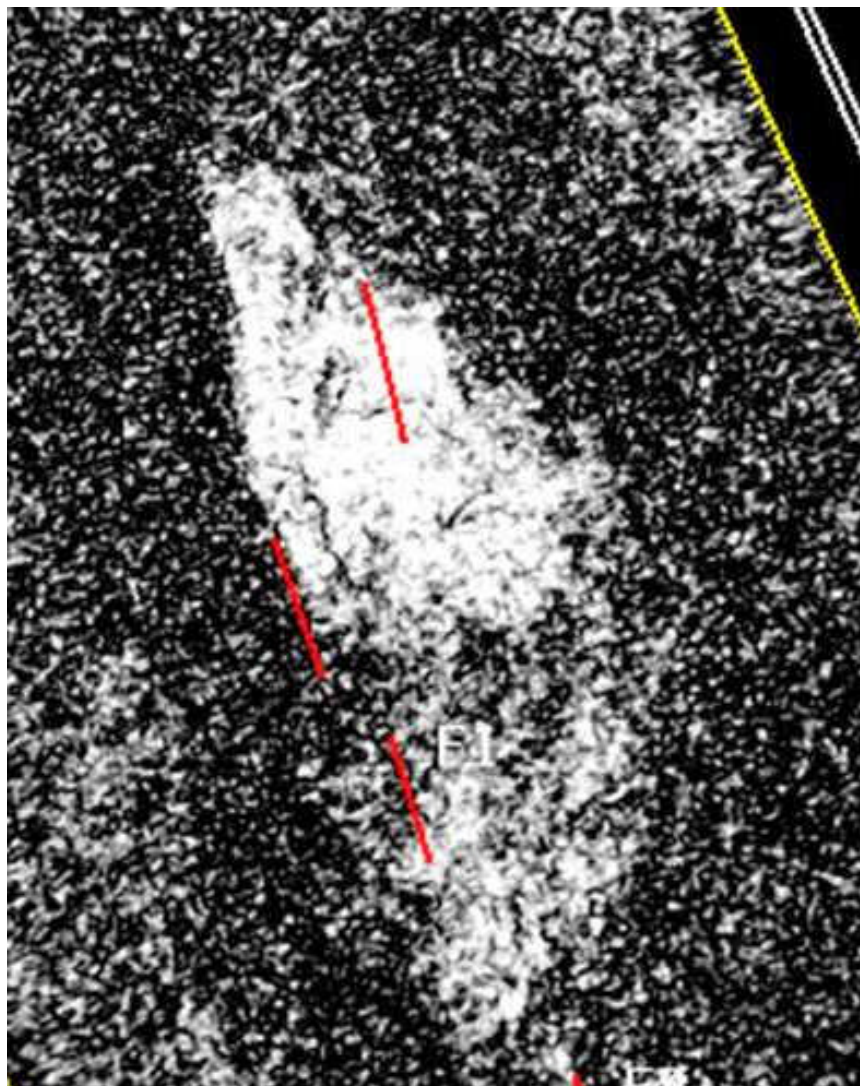
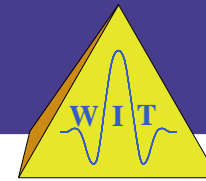
Conventional 3-D prestack depth migration
Courtesy of ENI E & P Division

Data example C

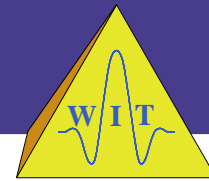
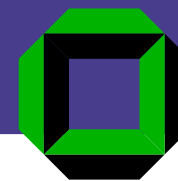


3-D poststack depth migration of CRS stack
Courtesy of ENI E & P Division

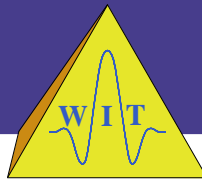
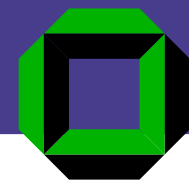
Data example C



depth slices of coherence images: conventional vs. CRS-based
Courtesy of ENI E & P Division

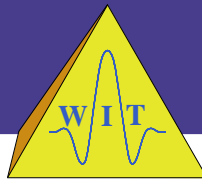
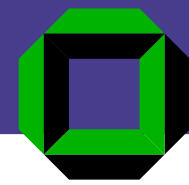


More data examples:
Presentation by Cardone et al.
Presentation by Trappe et al.
in this session



- Derive an approximation of the kinematic reflection response for a reflector segment in depth characterized by its

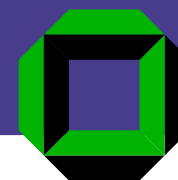
Basic concepts



- Derive an approximation of the kinematic reflection response for a reflector segment in depth characterized by its
 - local dip and
 - local curvature,



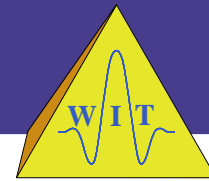
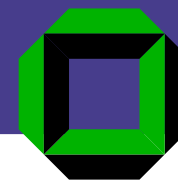
- Derive an approximation of the kinematic reflection response for a reflector segment in depth characterized by its
 - local dip and
 - local curvature,i. e., the reflector properties up to second order.



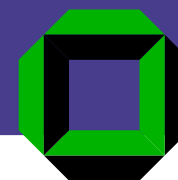
- Derive an approximation of the kinematic reflection response for a reflector segment in depth characterized by its
 - local dip and
 - local curvature,
i. e., the reflector properties up to second order.
- Use parameters defined either



- Derive an approximation of the kinematic reflection response for a reflector segment in depth characterized by its
 - local dip and
 - local curvature,
i. e., the reflector properties up to second order.
- Use parameters defined either
 - in the time domain
 - ↳ travelttime derivatives

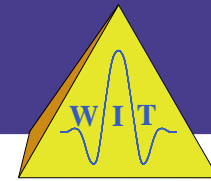


- Derive an approximation of the kinematic reflection response for a reflector segment in depth characterized by its
 - local dip and
 - local curvature,
i. e., the reflector properties up to second order.
- Use parameters defined either
 - in the time domain
 - ↳ traveltimes derivatives
 - or in the depth domain at the acquisition surface
 - ↳ properties of hypothetical wavefronts,



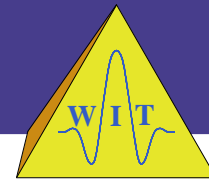
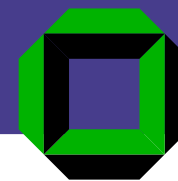
- Derive an approximation of the kinematic reflection response for a reflector segment in depth characterized by its
 - local dip and
 - local curvature,i. e., the reflector properties up to second order.
- Use parameters defined either
 - in the time domain
 - ↳ traveltimes derivatives
 - or in the depth domain at the acquisition surface
 - ↳ properties of hypothetical wavefronts,both linked by the near-surface velocity v_0 .

Basic concepts



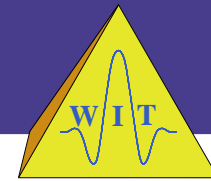
- Determine optimum stacking operator by means of coherence analysis in the data.
 - ↳ generalized multi-dimensional velocity analysis

Basic concepts



- Determine optimum stacking operator by means of coherence analysis in the data.
 - ↳ generalized multi-dimensional velocity analysis
- Stack along the determined stacking operator.

Basic concepts



- Determine optimum stacking operator by means of coherence analysis in the data.
 - ↳ generalized multi-dimensional velocity analysis
- Stack along the determined stacking operator.

Results:



- Determine optimum stacking operator by means of coherence analysis in the data.
 - ↳ generalized multi-dimensional velocity analysis
- Stack along the determined stacking operator.

Results:

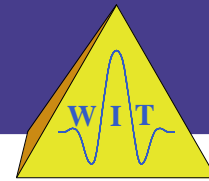
- a simulated section for an arbitrarily chosen configuration



- Determine optimum stacking operator by means of coherence analysis in the data.
 - ↳ generalized multi-dimensional velocity analysis
- Stack along the determined stacking operator.

Results:

- a simulated section for an arbitrarily chosen configuration
- a set of associated wavefield attribute sections



- Determine optimum stacking operator by means of coherence analysis in the data.
 - ↳ generalized multi-dimensional velocity analysis
- Stack along the determined stacking operator.

Results:

- a simulated section for an arbitrarily chosen configuration
- a set of associated wavefield attribute sections
 - ↳ subsequent applications like velocity determination



- Determine optimum stacking operator by means of coherence analysis in the data.
 - ↳ generalized multi-dimensional velocity analysis
- Stack along the determined stacking operator.

Results:

- a simulated section for an arbitrarily chosen configuration
- a set of associated wavefield attribute sections
 - ↳ subsequent applications like velocity determination
- an associated coherence section

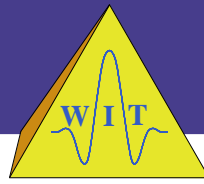
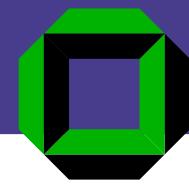


- Determine optimum stacking operator by means of coherence analysis in the data.
 - ↳ generalized multi-dimensional velocity analysis
- Stack along the determined stacking operator.

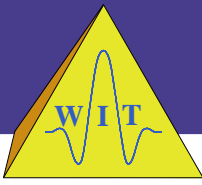
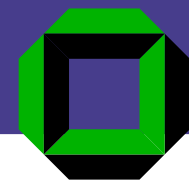
Results:

- a simulated section for an arbitrarily chosen configuration
- a set of associated wavefield attribute sections
 - ↳ subsequent applications like velocity determination
- an associated coherence section
 - ↳ identification of events, reliability of attributes

Derivation

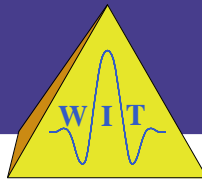
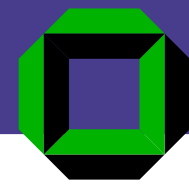


Possible ways to derive an approximation of the kinematic reflection response:



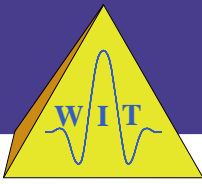
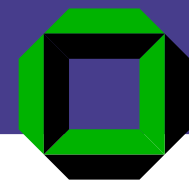
Possible ways to derive an approximation of the kinematic reflection response:

- paraxial ray theory, i. e., assumption of a linear relation between the properties of neighboring rays



Possible ways to derive an approximation of the kinematic reflection response:

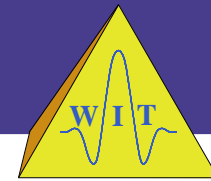
- paraxial ray theory, i. e., assumption of a linear relation between the properties of neighboring rays
- geometrical optics using the concept of object and image points (2-D case only)



Possible ways to derive an approximation of the kinematic reflection response:

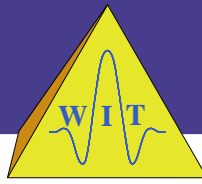
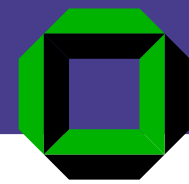
- paraxial ray theory, i. e., assumption of a linear relation between the properties of neighboring rays
- geometrical optics using the concept of object and image points (2-D case only)
- pragmatic way: second-order expansion of traveltime, initially without physical interpretation

Derivation



Prestack data:

(hyper-)volume $p(t, \vec{m}, \vec{h})$ with up to five dimensions



Prestack data:

(hyper-)volume $p(t, \vec{m}, \vec{h})$ with up to five dimensions

t

time

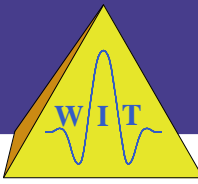
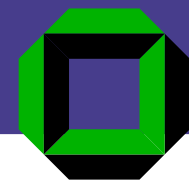
$$\vec{m} = \begin{pmatrix} m_x \\ m_y \end{pmatrix} = \frac{1}{2} \begin{pmatrix} g_x + s_x \\ g_y + s_y \end{pmatrix}$$

midpoint vector

$$\vec{h} = \begin{pmatrix} h_x \\ h_y \end{pmatrix} = \frac{1}{2} \begin{pmatrix} g_x - s_x \\ g_y - s_y \end{pmatrix}$$

half-offset vector

Derivation



Prestack data:

(hyper-)volume $p(t, \vec{m}, \vec{h})$ with up to five dimensions

t

time

$$\vec{m} = \begin{pmatrix} m_x \\ m_y \end{pmatrix} = \frac{1}{2} \begin{pmatrix} g_x + s_x \\ g_y + s_y \end{pmatrix}$$

midpoint vector

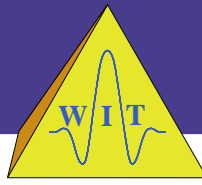
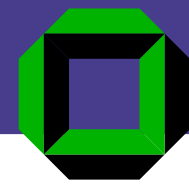
$$\vec{h} = \begin{pmatrix} h_x \\ h_y \end{pmatrix} = \frac{1}{2} \begin{pmatrix} g_x - s_x \\ g_y - s_y \end{pmatrix}$$

half-offset vector

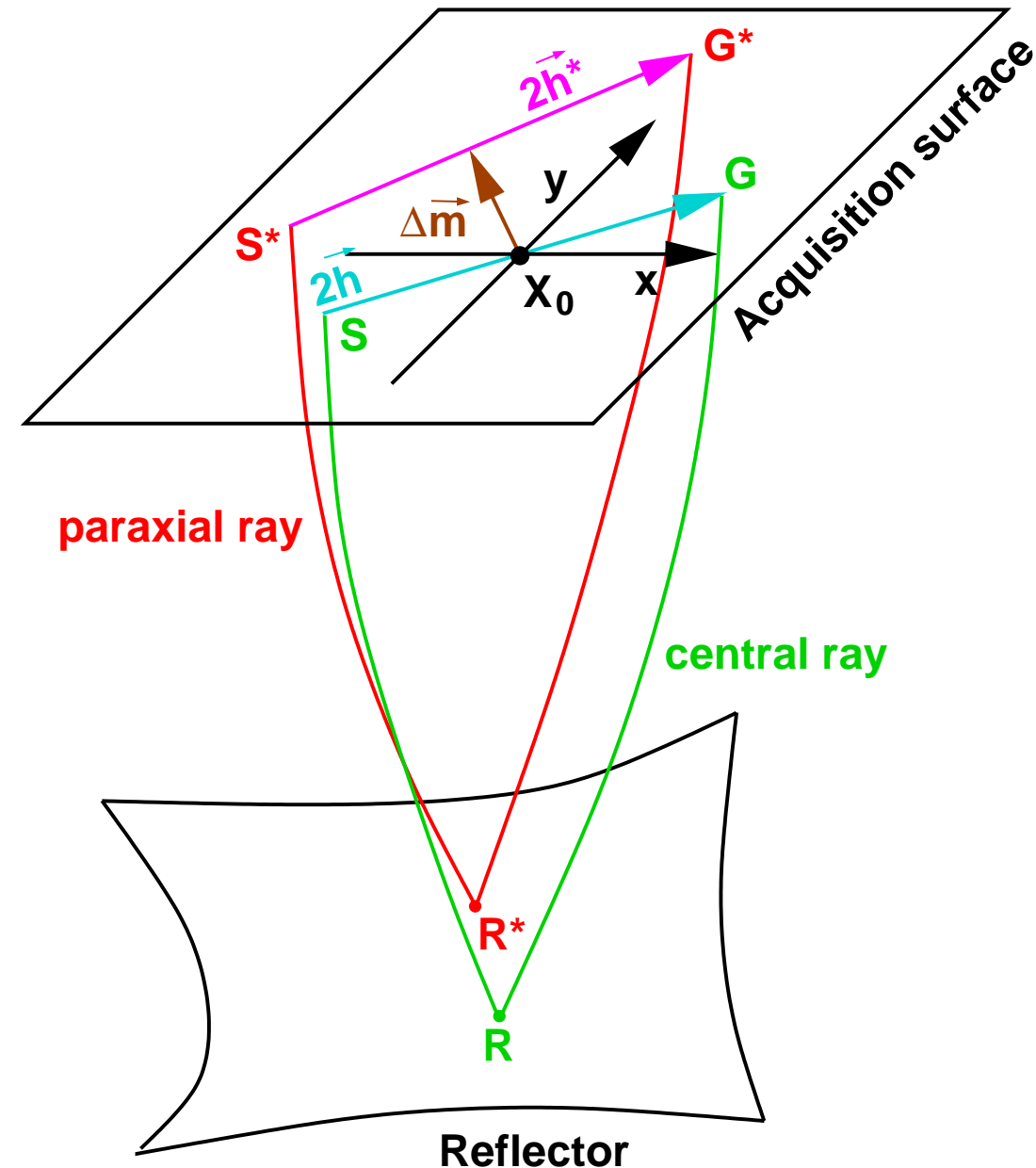
Reflection event:

(hyper-)surface $t(\vec{m}, \vec{h})$ in the prestack data

Central and paraxial rays

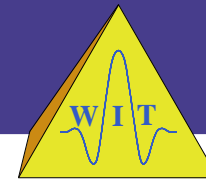


Assumed to be known:
traveltime $t(\vec{m}, \vec{h})$ along
central ray (SRG)



$$\Delta \vec{h} = \vec{h}^* - \vec{h}$$

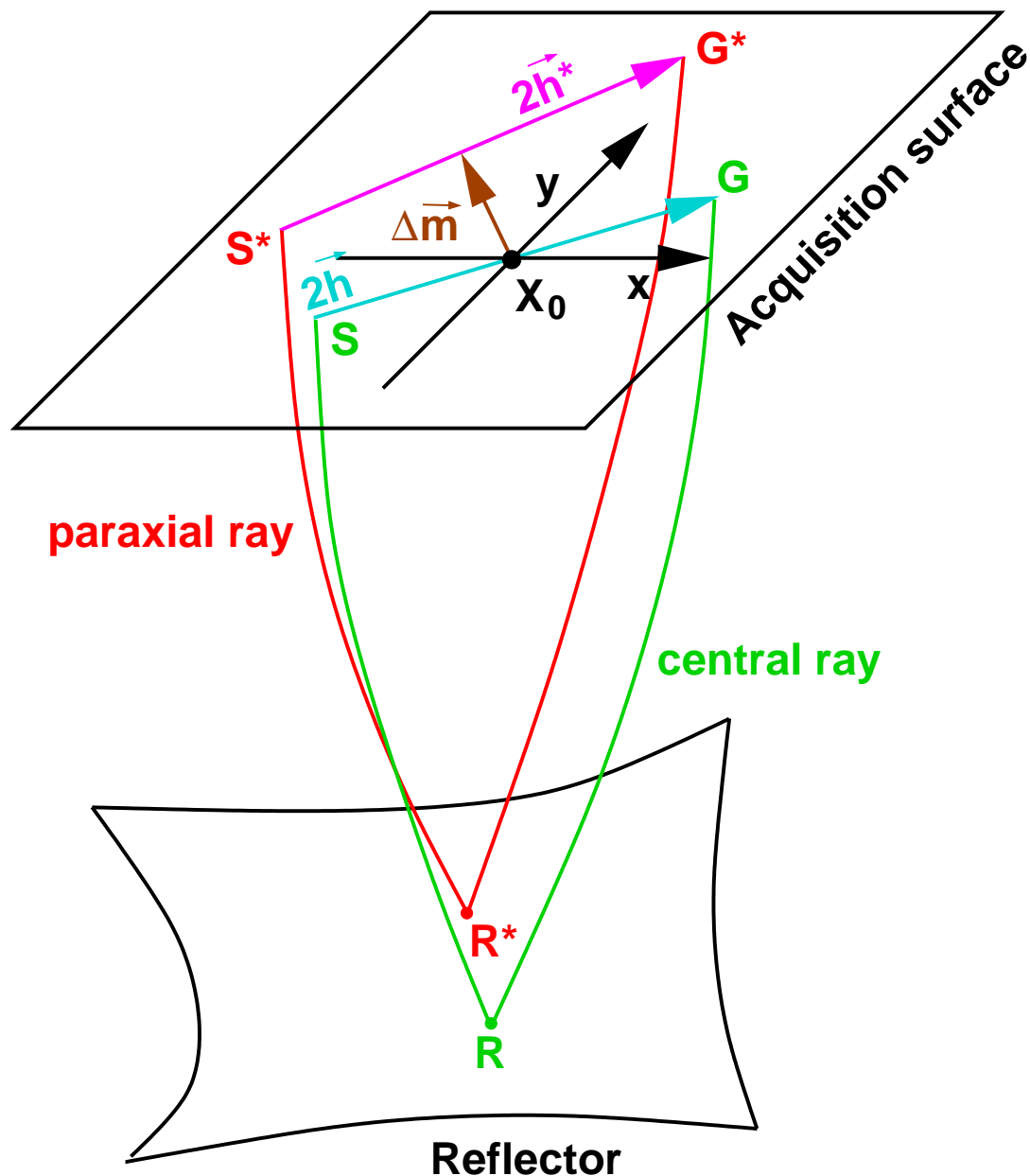
Central and paraxial rays



Assumed to be known:
traveltime $t(\vec{m}, \vec{h})$ along
central ray (SRG)

How to approximate
 $t(\vec{m} + \Delta\vec{m}, \vec{h} + \Delta\vec{h})$ along
paraxial ray (S*R*G*)?

$$\Delta\vec{h} = \vec{h}^* - \vec{h}$$



Central and paraxial rays

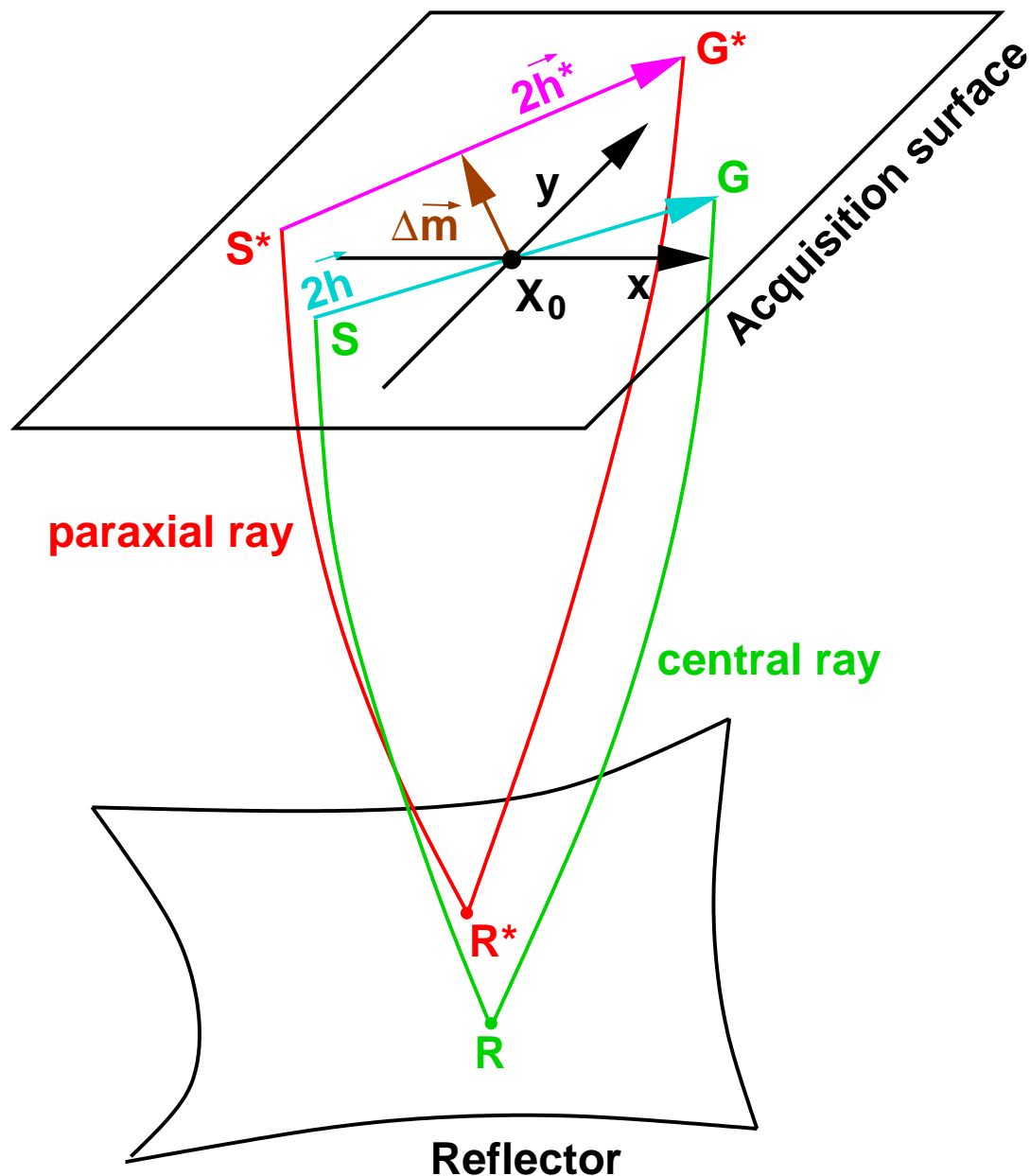


Assumed to be known:
traveltime $t(\vec{m}, \vec{h})$ along
central ray (SRG)

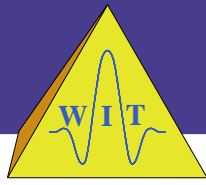
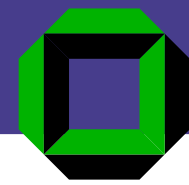
How to approximate
 $t(\vec{m} + \Delta\vec{m}, \vec{h} + \Delta\vec{h})$ along
paraxial ray (S*R*G*)?

→ Taylor expansion

$$\Delta\vec{h} = \vec{h}^* - \vec{h}$$

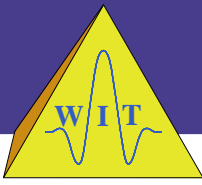
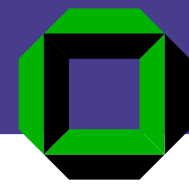


Pragmatic approach



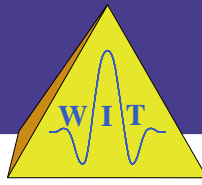
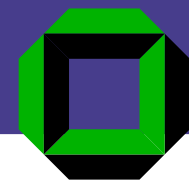
Taylor expansion up to second order – general case

Pragmatic approach



Taylor expansion up to second order – general case

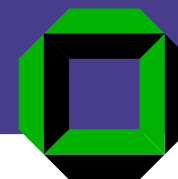
$$t(\vec{m} + \Delta\vec{m}, \vec{h} + \Delta\vec{h}) \approx$$



Taylor expansion up to second order – general case

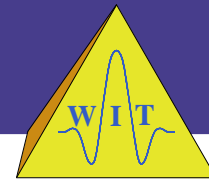
$$t(\vec{m} + \Delta\vec{m}, \vec{h} + \Delta\vec{h}) \approx$$
$$t(\vec{m}, \vec{h})$$

Pragmatic approach



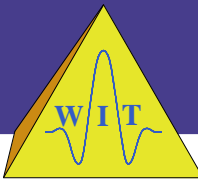
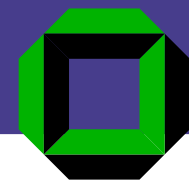
Taylor expansion up to second order – general case

$$t(\vec{m} + \Delta\vec{m}, \vec{h} + \Delta\vec{h}) \approx$$
$$t(\vec{m}, \vec{h}) + \frac{\partial t}{\partial m_x} \Delta m_x + \frac{\partial t}{\partial m_y} \Delta m_y + \frac{\partial t}{\partial h_x} \Delta h_x + \frac{\partial t}{\partial h_y} \Delta h_y$$



Taylor expansion up to second order – general case

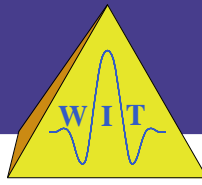
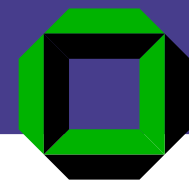
$$t(\vec{m} + \Delta\vec{m}, \vec{h} + \Delta\vec{h}) \approx$$
$$t(\vec{m}, \vec{h}) + \frac{\partial t}{\partial m_x} \Delta m_x + \frac{\partial t}{\partial m_y} \Delta m_y + \frac{\partial t}{\partial h_x} \Delta h_x + \frac{\partial t}{\partial h_y} \Delta h_y$$
$$+ \frac{1}{2} \left(\frac{\partial^2 t}{\partial m_x^2} \Delta m_x^2 + \frac{\partial^2 t}{\partial m_y^2} \Delta m_y^2 + \frac{\partial^2 t}{\partial h_x^2} \Delta h_x^2 + \frac{\partial^2 t}{\partial h_y^2} \Delta h_y^2 \right)$$



Taylor expansion up to second order – general case

$$\begin{aligned} t(\vec{m} + \Delta\vec{m}, \vec{h} + \Delta\vec{h}) &\approx \\ &t(\vec{m}, \vec{h}) + \frac{\partial t}{\partial m_x} \Delta m_x + \frac{\partial t}{\partial m_y} \Delta m_y + \frac{\partial t}{\partial h_x} \Delta h_x + \frac{\partial t}{\partial h_y} \Delta h_y \\ &+ \frac{1}{2} \left(\frac{\partial^2 t}{\partial m_x^2} \Delta m_x^2 + \frac{\partial^2 t}{\partial m_y^2} \Delta m_y^2 + \frac{\partial^2 t}{\partial h_x^2} \Delta h_x^2 + \frac{\partial^2 t}{\partial h_y^2} \Delta h_y^2 \right) \\ &+ \frac{\partial^2 t}{\partial m_x \partial m_y} \Delta m_x \Delta m_y + \frac{\partial^2 t}{\partial m_x \partial h_x} \Delta m_x \Delta h_x + \frac{\partial^2 t}{\partial m_x \partial h_y} \Delta m_x \Delta h_y \\ &+ \frac{\partial^2 t}{\partial m_y \partial h_x} \Delta m_y \Delta h_x + \frac{\partial^2 t}{\partial m_y \partial h_y} \Delta m_y \Delta h_y + \frac{\partial^2 t}{\partial h_x \partial h_y} \Delta h_x \Delta h_y \end{aligned}$$

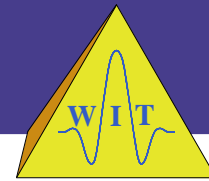
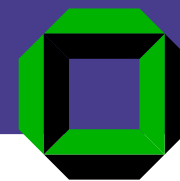
Pragmatic approach



Special case: Marine acquisition, single azimuth

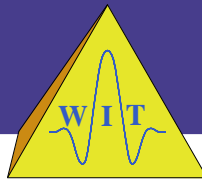
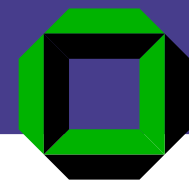
$$\begin{aligned} t(\vec{m} + \Delta\vec{m}, \vec{h} + \Delta\vec{h}) &\approx \\ t(\vec{m}, \vec{h}) &+ \frac{\partial t}{\partial m_x} \Delta m_x + \frac{\partial t}{\partial m_y} \Delta m_y + \frac{\partial t}{\partial h_x} \Delta h_x + \frac{\partial t}{\partial h_y} \Delta h_y \\ &+ \frac{1}{2} \left(\frac{\partial^2 t}{\partial m_x^2} \Delta m_x^2 + \frac{\partial^2 t}{\partial m_y^2} \Delta m_y^2 + \frac{\partial^2 t}{\partial h_x^2} \Delta h_x^2 + \frac{\partial^2 t}{\partial h_y^2} \Delta h_y^2 \right) \\ &+ \frac{\partial^2 t}{\partial m_x \partial m_y} \Delta m_x \Delta m_y + \frac{\partial^2 t}{\partial m_x \partial h_x} \Delta m_x \Delta h_x + \frac{\partial^2 t}{\partial m_x \partial h_y} \Delta m_x \Delta h_y \\ &+ \frac{\partial^2 t}{\partial m_y \partial h_x} \Delta m_y \Delta h_x + \frac{\partial^2 t}{\partial m_y \partial h_y} \Delta m_y \Delta h_y + \frac{\partial^2 t}{\partial h_x \partial h_y} \Delta h_x \Delta h_y \end{aligned}$$

Pragmatic approach



Special case: 2-D acquisition

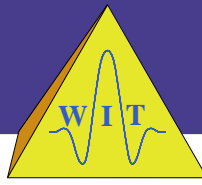
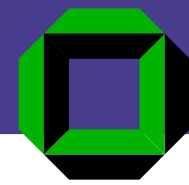
$$\begin{aligned} t(\vec{m} + \Delta\vec{m}, \vec{h} + \Delta\vec{h}) &\approx \\ t(\vec{m}, \vec{h}) &+ \frac{\partial t}{\partial m_x} \Delta m_x + \frac{\partial t}{\partial m_y} \Delta m_y + \frac{\partial t}{\partial h_x} \Delta h_x + \frac{\partial t}{\partial h_y} \Delta h_y \\ &+ \frac{1}{2} \left(\frac{\partial^2 t}{\partial m_x^2} \Delta m_x^2 + \frac{\partial^2 t}{\partial m_y^2} \Delta m_y^2 + \frac{\partial^2 t}{\partial h_x^2} \Delta h_x^2 + \frac{\partial^2 t}{\partial h_y^2} \Delta h_y^2 \right) \\ &+ \frac{\partial^2 t}{\partial m_x \partial m_y} \Delta m_x \Delta m_y + \frac{\partial^2 t}{\partial m_x \partial h_x} \Delta m_x \Delta h_x + \frac{\partial^2 t}{\partial m_x \partial h_y} \Delta m_x \Delta h_y \\ &+ \frac{\partial^2 t}{\partial m_y \partial h_x} \Delta m_y \Delta h_x + \frac{\partial^2 t}{\partial m_y \partial h_y} \Delta m_y \Delta h_y + \frac{\partial^2 t}{\partial h_x \partial h_y} \Delta h_x \Delta h_y \end{aligned}$$



General case

$$\begin{aligned} t(\vec{m} + \Delta\vec{m}, \vec{h} + \Delta\vec{h}) &\approx \\ t(\vec{m}, \vec{h}) &+ \frac{\partial t}{\partial m_x} \Delta m_x + \frac{\partial t}{\partial m_y} \Delta m_y + \frac{\partial t}{\partial h_x} \Delta h_x + \frac{\partial t}{\partial h_y} \Delta h_y \\ &+ \frac{1}{2} \left(\frac{\partial^2 t}{\partial m_x^2} \Delta m_x^2 + \frac{\partial^2 t}{\partial m_y^2} \Delta m_y^2 + \frac{\partial^2 t}{\partial h_x^2} \Delta h_x^2 + \frac{\partial^2 t}{\partial h_y^2} \Delta h_y^2 \right) \\ &+ \frac{\partial^2 t}{\partial m_x \partial m_y} \Delta m_x \Delta m_y + \frac{\partial^2 t}{\partial m_x \partial h_x} \Delta m_x \Delta h_x + \frac{\partial^2 t}{\partial m_x \partial h_y} \Delta m_x \Delta h_y \\ &+ \frac{\partial^2 t}{\partial m_y \partial h_x} \Delta m_y \Delta h_x + \frac{\partial^2 t}{\partial m_y \partial h_y} \Delta m_y \Delta h_y + \frac{\partial^2 t}{\partial h_x \partial h_y} \Delta h_x \Delta h_y \end{aligned}$$

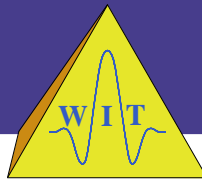
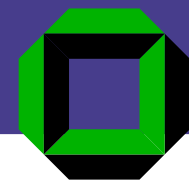
Pragmatic approach



Special case: zero-offset simulation

$$\begin{aligned} t(\vec{m} + \Delta\vec{m}, \vec{h} + \Delta\vec{h}) &\approx \\ t(\vec{m}, \vec{h}) &+ \frac{\partial t}{\partial m_x} \Delta m_x + \frac{\partial t}{\partial m_y} \Delta m_y + \frac{\partial t}{\partial h_x} \Delta h_x + \frac{\partial t}{\partial h_y} \Delta h_y \\ &+ \frac{1}{2} \left(\frac{\partial^2 t}{\partial m_x^2} \Delta m_x^2 + \frac{\partial^2 t}{\partial m_y^2} \Delta m_y^2 + \frac{\partial^2 t}{\partial h_x^2} \Delta h_x^2 + \frac{\partial^2 t}{\partial h_y^2} \Delta h_y^2 \right) \\ &+ \frac{\partial^2 t}{\partial m_x \partial m_y} \Delta m_x \Delta m_y + \frac{\partial^2 t}{\partial m_x \partial h_x} \Delta m_x \Delta h_x + \frac{\partial^2 t}{\partial m_x \partial h_y} \Delta m_x \Delta h_y \\ &+ \frac{\partial^2 t}{\partial m_y \partial h_x} \Delta m_y \Delta h_x + \frac{\partial^2 t}{\partial m_y \partial h_y} \Delta m_y \Delta h_y + \frac{\partial^2 t}{\partial h_x \partial h_y} \Delta h_x \Delta h_y \end{aligned}$$

Pragmatic approach



Special case: zero-offset simulation, marine case

$$t(\vec{m} + \Delta\vec{m}, \vec{h} + \Delta\vec{h}) \approx$$

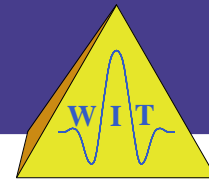
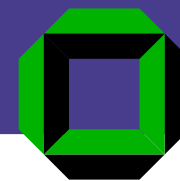
$$t(\vec{m}, \vec{h}) + \frac{\partial t}{\partial m_x} \Delta m_x + \frac{\partial t}{\partial m_y} \Delta m_y + \frac{\partial t}{\partial h_x} \Delta h_x + \frac{\partial t}{\partial h_y} \Delta h_y$$

$$+ \frac{1}{2} \left(\frac{\partial^2 t}{\partial m_x^2} \Delta m_x^2 + \frac{\partial^2 t}{\partial m_y^2} \Delta m_y^2 + \frac{\partial^2 t}{\partial h_x^2} \Delta h_x^2 + \frac{\partial^2 t}{\partial h_y^2} \Delta h_y^2 \right)$$

$$+ \frac{\partial^2 t}{\partial m_x \partial m_y} \Delta m_x \Delta m_y + \frac{\partial^2 t}{\partial m_x \partial h_x} \Delta m_x \Delta h_x + \frac{\partial^2 t}{\partial m_x \partial h_y} \Delta m_x \Delta h_y$$

$$+ \frac{\partial^2 t}{\partial m_y \partial h_x} \Delta m_y \Delta h_x + \frac{\partial^2 t}{\partial m_y \partial h_y} \Delta m_y \Delta h_y + \frac{\partial^2 t}{\partial h_x \partial h_y} \Delta h_x \Delta h_y$$

Pragmatic approach



Special case: zero-offset simulation, 2-D acquisition

$$t(\vec{m} + \Delta\vec{m}, \vec{h} + \Delta\vec{h}) \approx$$

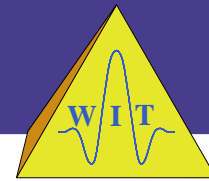
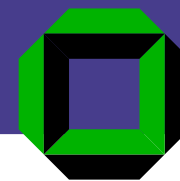
$$t(\vec{m}, \vec{h}) + \frac{\partial t}{\partial m_x} \Delta m_x + \frac{\partial t}{\partial m_y} \Delta m_y + \frac{\partial t}{\partial h_x} \Delta h_x + \frac{\partial t}{\partial h_y} \Delta h_y$$

$$+ \frac{1}{2} \left(\frac{\partial^2 t}{\partial m_x^2} \Delta m_x^2 + \frac{\partial^2 t}{\partial m_y^2} \Delta m_y^2 + \frac{\partial^2 t}{\partial h_x^2} \Delta h_x^2 + \frac{\partial^2 t}{\partial h_y^2} \Delta h_y^2 \right)$$

$$+ \frac{\partial^2 t}{\partial m_x \partial m_y} \Delta m_x \Delta m_y + \frac{\partial^2 t}{\partial m_x \partial h_x} \Delta m_x \Delta h_x + \frac{\partial^2 t}{\partial m_x \partial h_y} \Delta m_x \Delta h_y$$

$$+ \frac{\partial^2 t}{\partial m_y \partial h_x} \Delta m_y \Delta h_x + \frac{\partial^2 t}{\partial m_y \partial h_y} \Delta m_y \Delta h_y + \frac{\partial^2 t}{\partial h_x \partial h_y} \Delta h_x \Delta h_y$$

Pragmatic approach



Special case: ZO simulation, 2-D, CMP gathers only

$$t(\vec{m} + \Delta\vec{m}, \vec{h} + \Delta\vec{h}) \approx$$

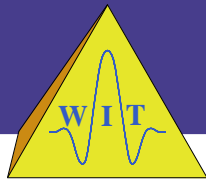
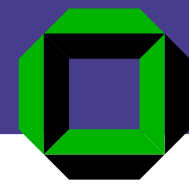
$$t(\vec{m}, \vec{h}) + \frac{\partial t}{\partial m_x} \Delta m_x + \frac{\partial t}{\partial m_y} \Delta m_y + \frac{\partial t}{\partial h_x} \Delta h_x + \frac{\partial t}{\partial h_y} \Delta h_y$$

$$+ \frac{1}{2} \left(\frac{\partial^2 t}{\partial m_x^2} \Delta m_x^2 + \frac{\partial^2 t}{\partial m_y^2} \Delta m_y^2 + \frac{\partial^2 t}{\partial h_x^2} \Delta h_x^2 + \frac{\partial^2 t}{\partial h_y^2} \Delta h_y^2 \right)$$

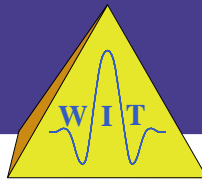
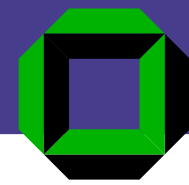
$$+ \frac{\partial^2 t}{\partial m_x \partial m_y} \Delta m_x \Delta m_y + \frac{\partial^2 t}{\partial m_x \partial h_x} \Delta m_x \Delta h_x + \frac{\partial^2 t}{\partial m_x \partial h_y} \Delta m_x \Delta h_y$$

$$+ \frac{\partial^2 t}{\partial m_y \partial h_x} \Delta m_y \Delta h_x + \frac{\partial^2 t}{\partial m_y \partial h_y} \Delta m_y \Delta h_y + \frac{\partial^2 t}{\partial h_x \partial h_y} \Delta h_x \Delta h_y$$

Pragmatic approach



Preliminary conclusions:



Preliminary conclusions:

- In some cases, not all derivatives are independent in the context of paraxial ray theory. This is not evident at this stage!



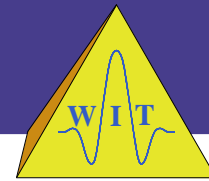
Preliminary conclusions:

- In some cases, not all derivatives are independent in the context of paraxial ray theory. This is not evident at this stage!
- Hyperbolic approximations can be obtained by squaring and neglecting higher order terms.



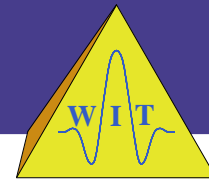
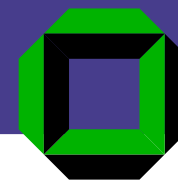
Preliminary conclusions:

- In some cases, not all derivatives are independent in the context of paraxial ray theory. This is not evident at this stage!
- Hyperbolic approximations can be obtained by squaring and neglecting higher order terms.
- We need a physical interpretation of the derivatives



Preliminary conclusions:

- In some cases, not all derivatives are independent in the context of paraxial ray theory. This is not evident at this stage!
- Hyperbolic approximations can be obtained by squaring and neglecting higher order terms.
- We need a physical interpretation of the derivatives
 - to identify hidden dependencies,



Preliminary conclusions:

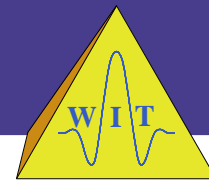
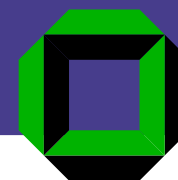
- In some cases, not all derivatives are independent in the context of paraxial ray theory. This is not evident at this stage!
- Hyperbolic approximations can be obtained by squaring and neglecting higher order terms.
- We need a physical interpretation of the derivatives
 - to identify hidden dependencies,
 - to understand which values are physically reasonable,



Preliminary conclusions:

- In some cases, not all derivatives are independent in the context of paraxial ray theory. This is not evident at this stage!
- Hyperbolic approximations can be obtained by squaring and neglecting higher order terms.
- We need a physical interpretation of the derivatives
 - to identify hidden dependencies,
 - to understand which values are physically reasonable,
 - and to make use of the derivatives for various purposes.

Physical interpretation



Simplest case: 2-D acquisition, zero-offset

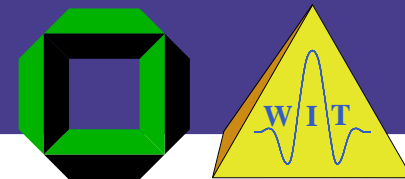
$$t(x_m, h) = t_0 + \frac{\partial t}{\partial x_m} (x_m - x_0) + \frac{1}{2} \left[\frac{\partial^2 t}{\partial x_m^2} (x_m - x_0)^2 + \frac{\partial^2 t}{\partial h^2} h^2 \right]$$



Simplest case: 2-D acquisition, zero-offset

$$t(x_m, h) = t_0 + \frac{\partial t}{\partial x_m} (x_m - x_0) + \frac{1}{2} \left[\frac{\partial^2 t}{\partial x_m^2} (x_m - x_0)^2 + \frac{\partial^2 t}{\partial h^2} h^2 \right]$$

Physical interpretation

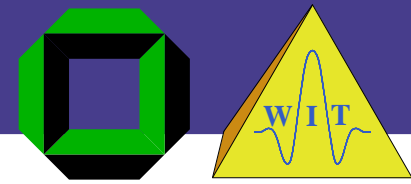


Simplest case: 2-D acquisition, zero-offset

$$t(x_m, h) = t_0 + \frac{\partial t}{\partial x_m} (x_m - x_0) + \frac{1}{2} \left[\frac{\partial^2 t}{\partial x_m^2} (x_m - x_0)^2 + \frac{\partial^2 t}{\partial h^2} h^2 \right]$$

Horizontal slowness:

$$p_x = \frac{1}{2} \frac{\partial t}{\partial x_m} \Big|_{(x_m=x_0, h=0)}$$



Simplest case: 2-D acquisition, zero-offset

$$t(x_m, h) = t_0 + \frac{\partial t}{\partial x_m} (x_m - x_0) + \frac{1}{2} \left[\frac{\partial^2 t}{\partial x_m^2} (x_m - x_0)^2 + \frac{\partial^2 t}{\partial h^2} h^2 \right]$$

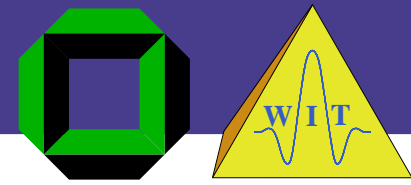
Horizontal slowness:

$$p_x = \frac{1}{2} \frac{\partial t}{\partial x_m} \Big|_{(x_m=x_0, h=0)} = |\vec{p}| \sin \alpha$$

\vec{p} slowness vector

α emergence angle

v_0 near-surface velocity



Simplest case: 2-D acquisition, zero-offset

$$t(x_m, h) = t_0 + \frac{\partial t}{\partial x_m} (x_m - x_0) + \frac{1}{2} \left[\frac{\partial^2 t}{\partial x_m^2} (x_m - x_0)^2 + \frac{\partial^2 t}{\partial h^2} h^2 \right]$$

Horizontal slowness:

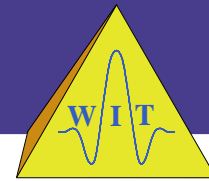
$$p_x = \frac{1}{2} \frac{\partial t}{\partial x_m} \Bigg|_{(x_m=x_0, h=0)} = |\vec{p}| \sin \alpha = \frac{\sin \alpha}{v_0}$$

\vec{p} slowness vector

α emergence angle

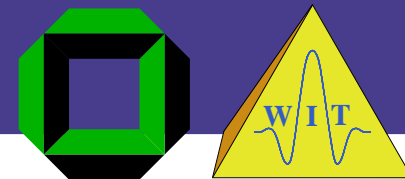
v_0 near-surface velocity

Physical interpretation



Simplest case: 2-D acquisition, zero-offset

$$t(x_m, h) = t_0 + \frac{\partial t}{\partial x_m} (x_m - x_0) + \frac{1}{2} \left[\frac{\partial^2 t}{\partial x_m^2} (x_m - x_0)^2 + \frac{\partial^2 t}{\partial h^2} h^2 \right]$$

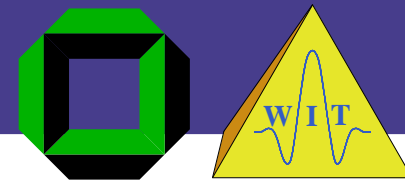


Simplest case: 2-D acquisition, zero-offset

$$t(x_m, h) = t_0 + \frac{\partial t}{\partial x_m} (x_m - x_0) + \frac{1}{2} \left[\frac{\partial^2 t}{\partial x_m^2} (x_m - x_0)^2 + \frac{\partial^2 t}{\partial h^2} h^2 \right]$$

Curvature of “zero-offset wavefront”:

$$K_N = \left. \frac{\partial^2 t}{\partial x_m^2} \right|_{(x_m=x_0, h=0)}$$

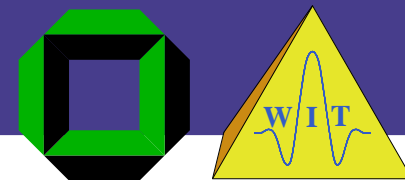


Simplest case: 2-D acquisition, zero-offset

$$t(x_m, h) = t_0 + \frac{\partial t}{\partial x_m} (x_m - x_0) + \frac{1}{2} \left[\frac{\partial^2 t}{\partial x_m^2} (x_m - x_0)^2 + \frac{\partial^2 t}{\partial h^2} h^2 \right]$$

Curvature of “zero-offset wavefront”:

$$K_N = \frac{v_0}{2} \left. \frac{\partial^2 t}{\partial x_m^2} \right|_{(x_m=x_0, h=0)}$$

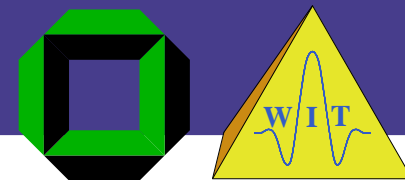


Simplest case: 2-D acquisition, zero-offset

$$t(x_m, h) = t_0 + \frac{\partial t}{\partial x_m} (x_m - x_0) + \frac{1}{2} \left[\frac{\partial^2 t}{\partial x_m^2} (x_m - x_0)^2 + \frac{\partial^2 t}{\partial h^2} h^2 \right]$$

Curvature of “zero-offset wavefront”:

$$K_N = \frac{v_0}{2} \frac{1}{\cos^2 \alpha} \frac{\partial^2 t}{\partial x_m^2} \Big|_{(x_m=x_0, h=0)}$$



Simplest case: 2-D acquisition, zero-offset

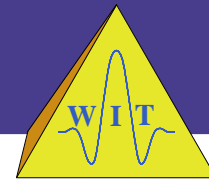
$$t(x_m, h) = t_0 + \frac{\partial t}{\partial x_m} (x_m - x_0) + \frac{1}{2} \left[\frac{\partial^2 t}{\partial x_m^2} (x_m - x_0)^2 + \frac{\partial^2 t}{\partial h^2} h^2 \right]$$

Curvature of “zero-offset wavefront”:

$$K_N = \frac{v_0}{2} \frac{1}{\cos^2 \alpha} \frac{\partial^2 t}{\partial x_m^2} \Bigg|_{(x_m=x_0, h=0)}$$

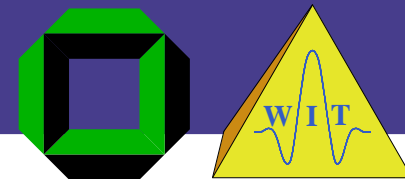
A “zero-offset wavefront”, also called normal wavefront, can be obtained from an exploding reflector experiment.

Physical interpretation



Simplest case: 2-D acquisition, zero-offset

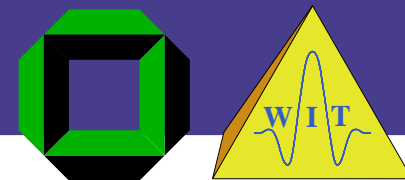
$$t(x_m, h) = t_0 + \frac{\partial t}{\partial x_m} (x_m - x_0) + \frac{1}{2} \left[\frac{\partial^2 t}{\partial x_m^2} (x_m - x_0)^2 + \frac{\partial^2 t}{\partial h^2} h^2 \right]$$



Simplest case: 2-D acquisition, zero-offset

$$t(x_m, h) = t_0 + \frac{\partial t}{\partial x_m} (x_m - x_0) + \frac{1}{2} \left[\frac{\partial^2 t}{\partial x_m^2} (x_m - x_0)^2 + \frac{\partial^2 t}{\partial h^2} h^2 \right]$$

Curvature of “common-midpoint (CMP) wavefront”:

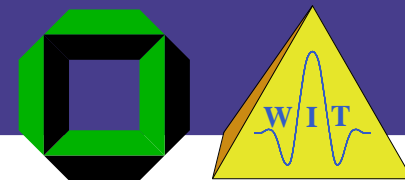


Simplest case: 2-D acquisition, zero-offset

$$t(x_m, h) = t_0 + \frac{\partial t}{\partial x_m} (x_m - x_0) + \frac{1}{2} \left[\frac{\partial^2 t}{\partial x_m^2} (x_m - x_0)^2 + \frac{\partial^2 t}{\partial h^2} h^2 \right]$$

Curvature of “common-midpoint (CMP) wavefront”:

Problem: no simple physical experiment available!



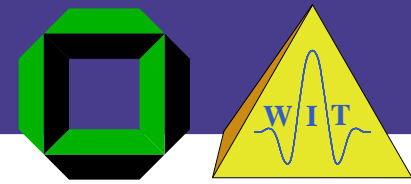
Simplest case: 2-D acquisition, zero-offset

$$t(x_m, h) = t_0 + \frac{\partial t}{\partial x_m} (x_m - x_0) + \frac{1}{2} \left[\frac{\partial^2 t}{\partial x_m^2} (x_m - x_0)^2 + \frac{\partial^2 t}{\partial h^2} h^2 \right]$$

Curvature of “common-midpoint (CMP) wavefront”:

Problem: no simple physical experiment available!

However: up to second order, CMP traveltimes and zero-offset diffraction traveltimes coincide (NIP wave theorem, Hubral 1983).



Simplest case: 2-D acquisition, zero-offset

$$t(x_m, h) = t_0 + \frac{\partial t}{\partial x_m} (x_m - x_0) + \frac{1}{2} \left[\frac{\partial^2 t}{\partial x_m^2} (x_m - x_0)^2 + \frac{\partial^2 t}{\partial h^2} h^2 \right]$$

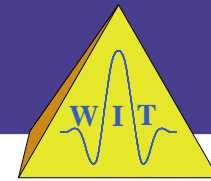
Curvature of “common-midpoint (CMP) wavefront”:

Problem: no simple physical experiment available!

However: up to second order, CMP traveltimes and zero-offset diffraction traveltimes coincide (NIP wave theorem, Hubral 1983).

➡ In analogy to the exploding reflector experiment, an exploding reflection point experiment approximates the “CMP wavefront”.

Physical interpretation

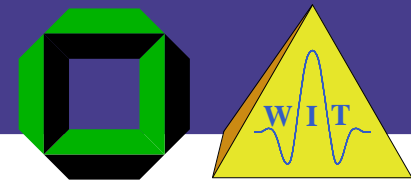


Simplest case: 2-D acquisition, zero-offset

$$t(x_m, h) = t_0 + \frac{\partial t}{\partial x_m} (x_m - x_0) + \frac{1}{2} \left[\frac{\partial^2 t}{\partial x_m^2} (x_m - x_0)^2 + \frac{\partial^2 t}{\partial h^2} h^2 \right]$$

Curvature of “common-midpoint (CMP) wavefront”:

$$K_{NIP} = \frac{1}{2} \frac{v_0}{\cos^2 \alpha} \frac{\partial^2 t}{\partial h^2} \Bigg|_{(x_m=x_0, h=0)}$$



Simplest case: 2-D acquisition, zero-offset

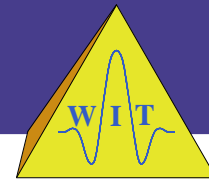
$$t(x_m, h) = t_0 + \frac{\partial t}{\partial x_m} (x_m - x_0) + \frac{1}{2} \left[\frac{\partial^2 t}{\partial x_m^2} (x_m - x_0)^2 + \frac{\partial^2 t}{\partial h^2} h^2 \right]$$

Curvature of “common-midpoint (CMP) wavefront”:

$$K_{NIP} = \frac{1}{2} \frac{v_0}{\cos^2 \alpha} \frac{\partial^2 t}{\partial h^2} \Bigg|_{(x_m=x_0, h=0)}$$

An exploding reflection-point experiment yields the so-called normal-incidence-point (NIP) wavefront.

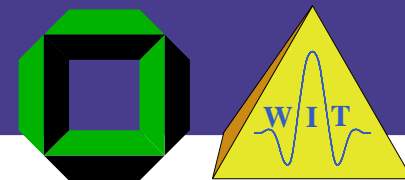
Physical interpretation



Replacing all derivatives, we obtain

$$t(x_m, h) = t_0 + \frac{2 \sin \alpha}{v_0} (x_m - x_0) + \frac{\cos^2 \alpha}{v_0} \left[K_N (x_m - x_0) + K_{NIP} h^2 \right]$$

in terms of *kinematic wavefield attributes*.



Replacing all derivatives, we obtain

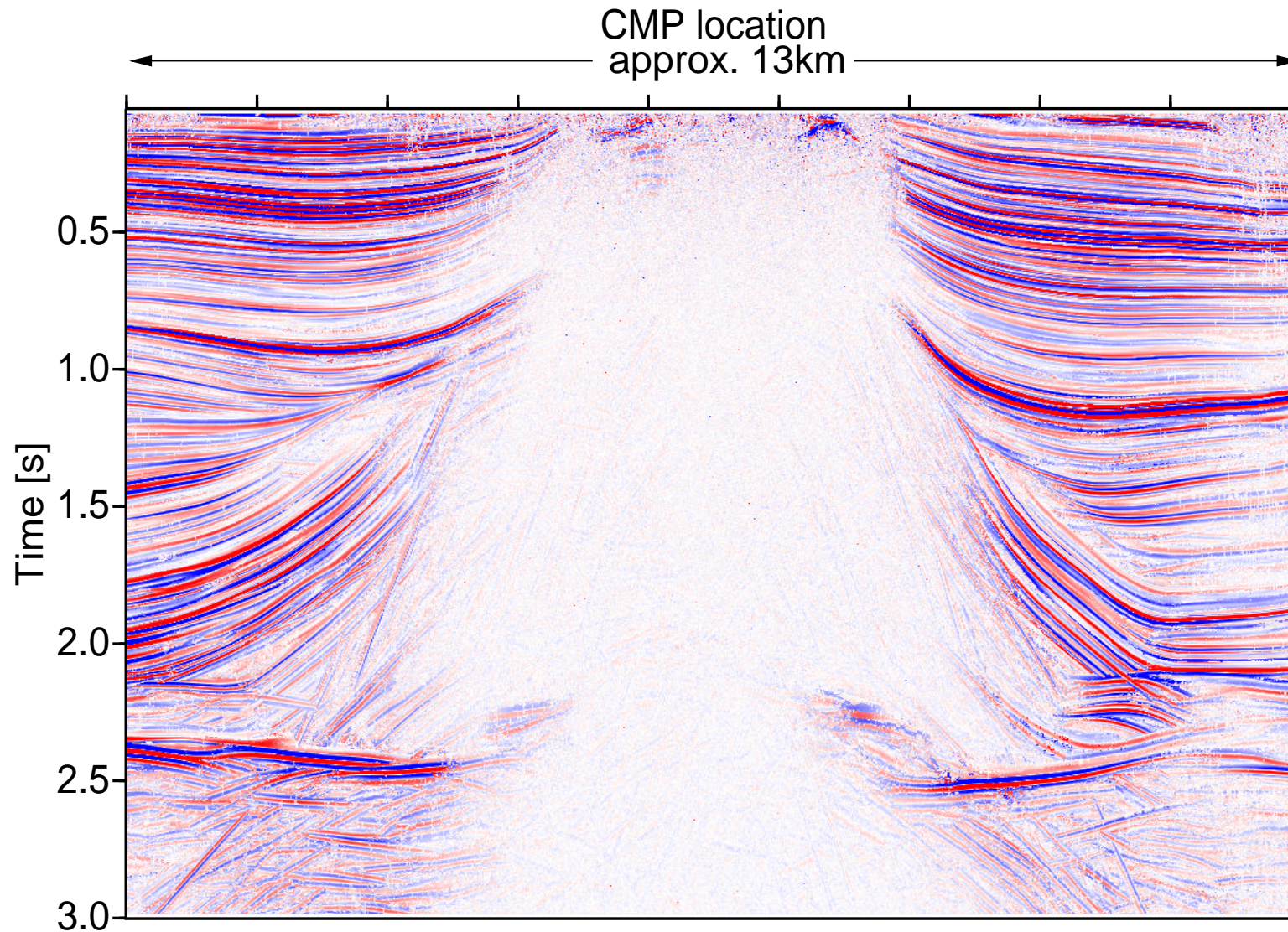
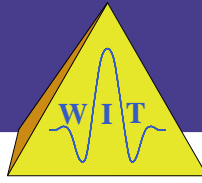
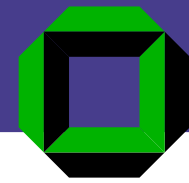
$$t(x_m, h) = t_0 + \frac{2 \sin \alpha}{v_0} (x_m - x_0) + \frac{\cos^2 \alpha}{v_0} \left[K_N (x_m - x_0) + K_{NIP} h^2 \right]$$

in terms of *kinematic wavefield attributes*.

Accordingly, the hyperbolic counterpart reads

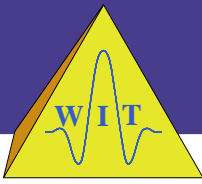
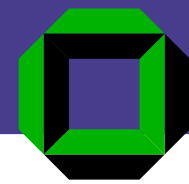
$$t^2(x_m, h) \approx \tilde{t}^2(x_m, h) = \left[t_0 + \frac{2 \sin \alpha}{v_0} (x_m - x_0) \right]^2 + \frac{2 t_0 \cos^2 \alpha}{v_0} \left[K_N (x_m - x_0)^2 + K_{NIP} h^2 \right].$$

Data example A

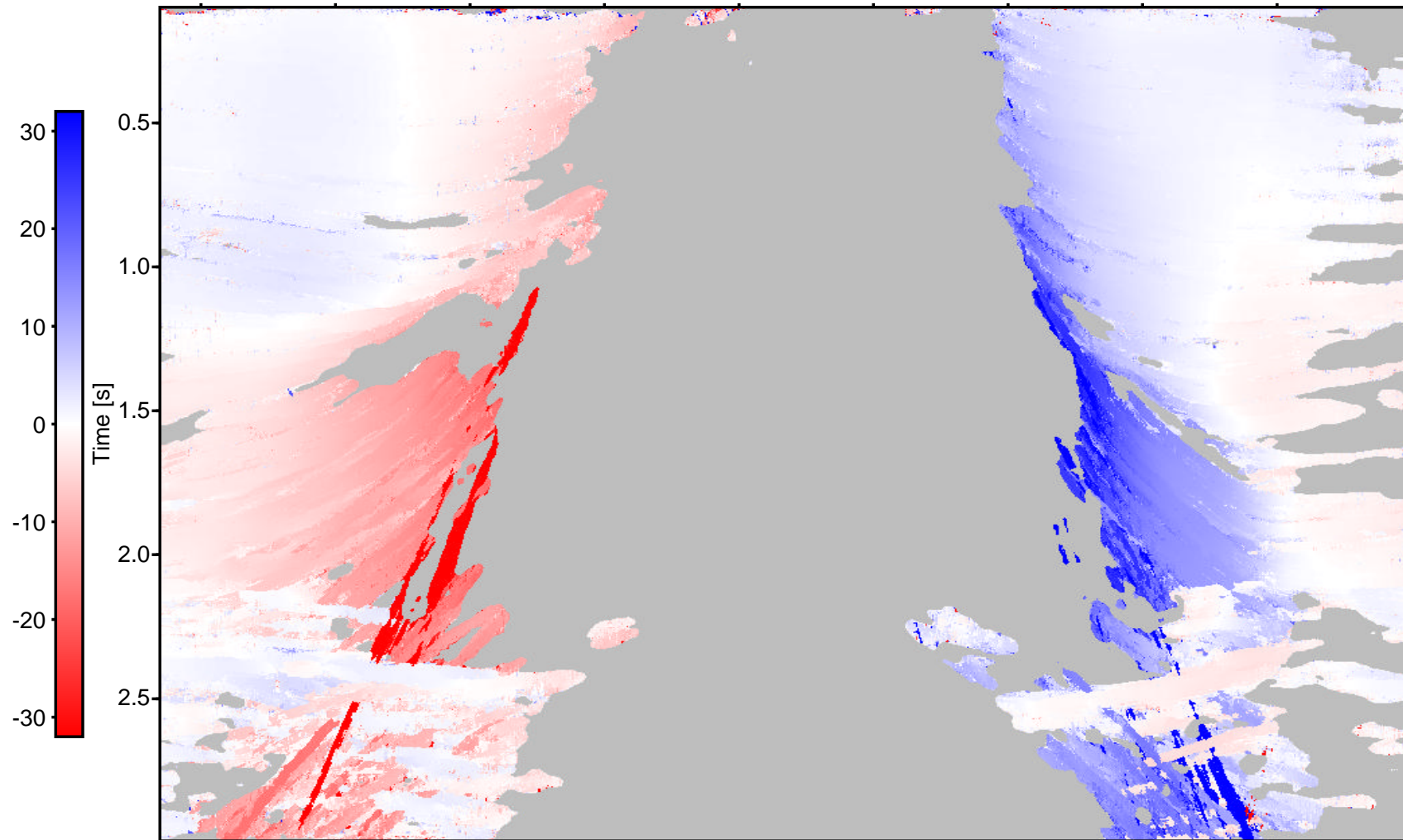


2-D CRS stack – from Müller (1999)

Data example A

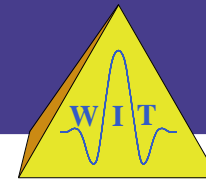


CMP

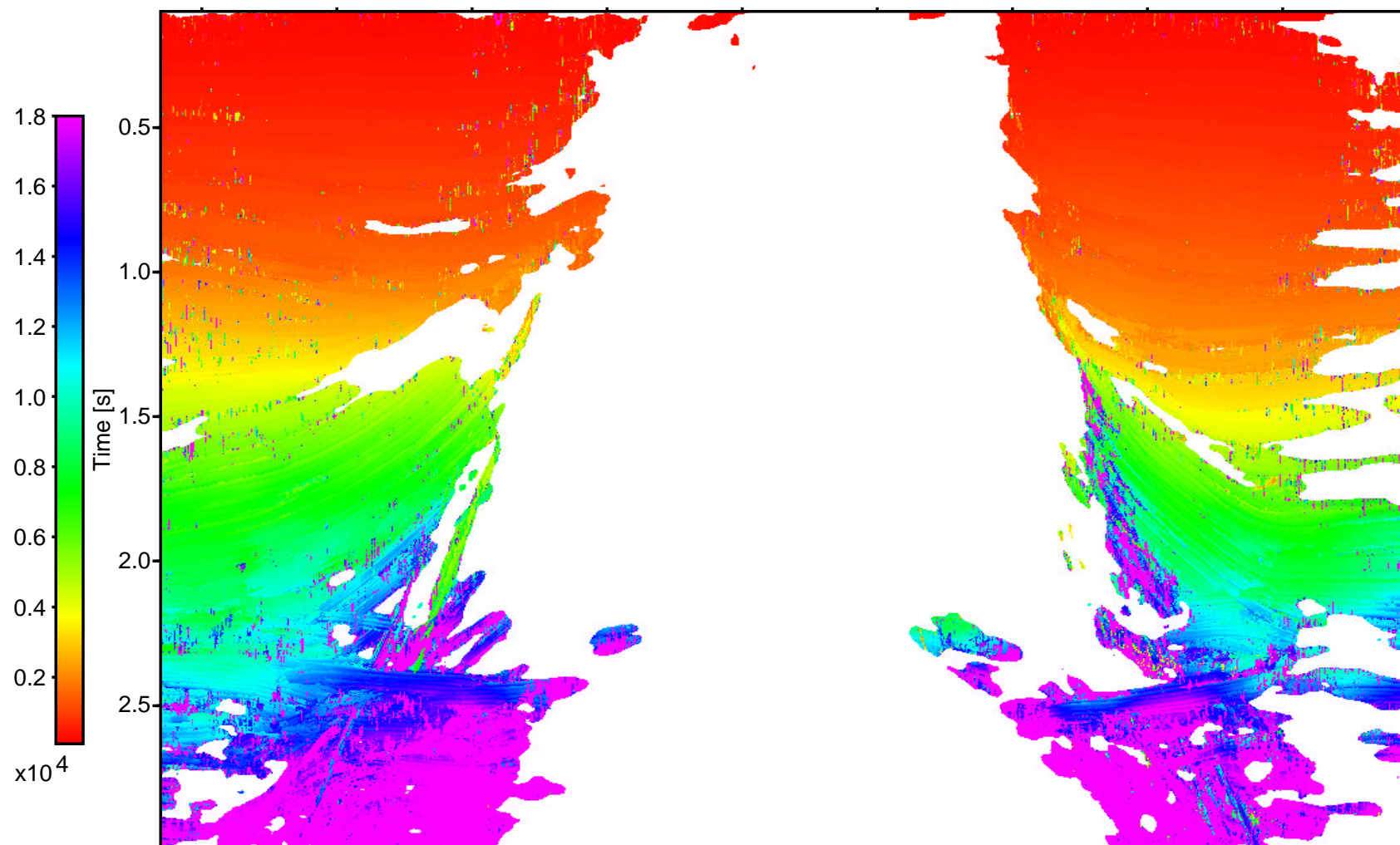


Emergence angle α [°]

Data example A



CMP

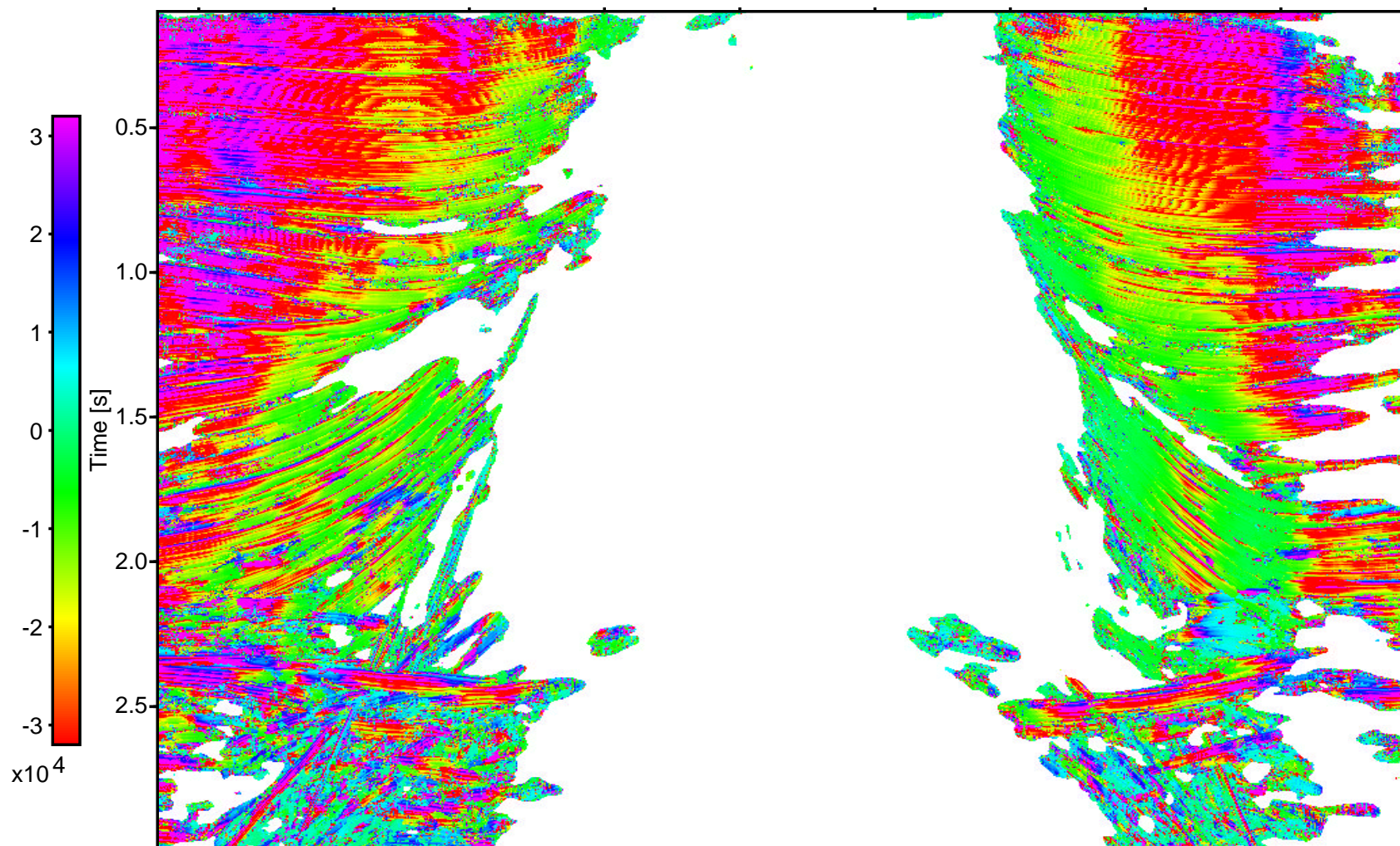


Radius of curvature of NIP wavefront [m]

Data example A

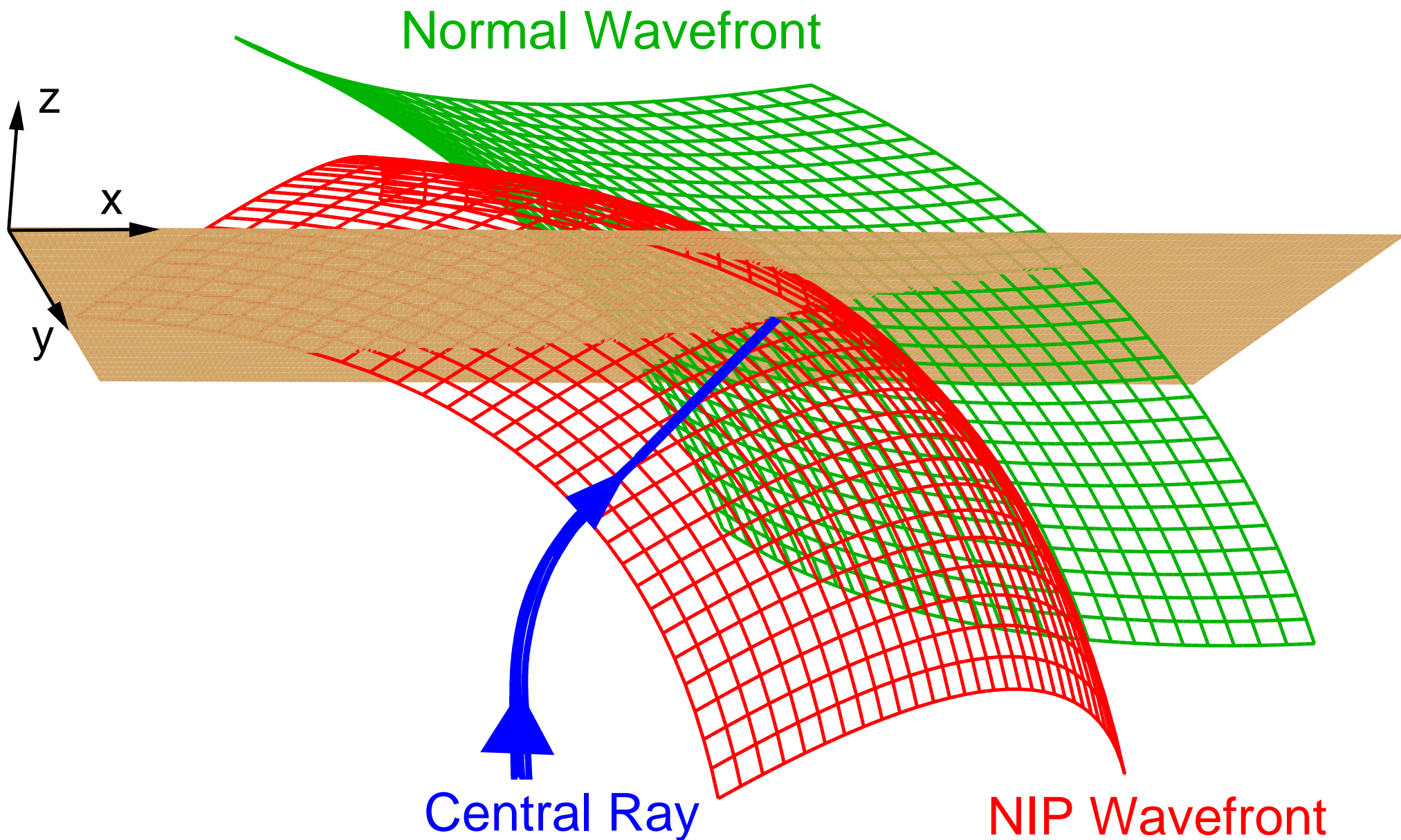


CMP

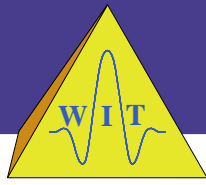
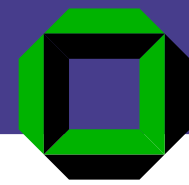


Radius of curvature of normal wavefront [m]

From 2-D to 3-D

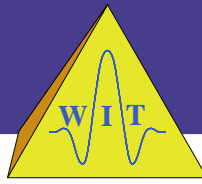
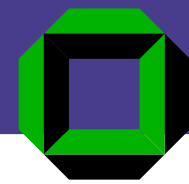


From 2-D to 3-D



From scalar curvatures to curvature matrices:

From 2-D to 3-D

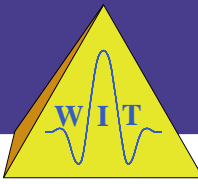
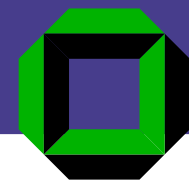


From scalar curvatures to curvature matrices:

$$K_{NIP} \mapsto \mathbf{K}_{NIP} = \frac{v_0}{2} \mathbf{T}^T \begin{pmatrix} \frac{\partial^2 t}{\partial h_x^2} & \frac{\partial^2 t}{\partial h_x \partial h_y} \\ \frac{\partial^2 t}{\partial h_y \partial h_x} & \frac{\partial^2 t}{\partial h_y^2} \end{pmatrix} \mathbf{T}$$

$$K_N \mapsto \mathbf{K}_N = \frac{v_0}{2} \mathbf{T}^T \begin{pmatrix} \frac{\partial^2 t}{\partial m_x^2} & \frac{\partial^2 t}{\partial m_x \partial m_y} \\ \frac{\partial^2 t}{\partial m_y \partial m_x} & \frac{\partial^2 t}{\partial m_y^2} \end{pmatrix} \mathbf{T}$$

From 2-D to 3-D



From scalar curvatures to curvature matrices:

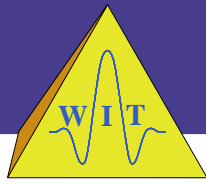
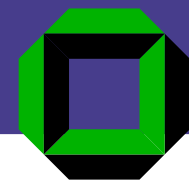
$$K_{NIP} \mapsto \mathbf{K}_{NIP} = \frac{v_0}{2} \mathbf{T}^T \begin{pmatrix} \frac{\partial^2 t}{\partial h_x^2} & \frac{\partial^2 t}{\partial h_x \partial h_y} \\ \frac{\partial^2 t}{\partial h_y \partial h_x} & \frac{\partial^2 t}{\partial h_y^2} \end{pmatrix} \mathbf{T}$$

$$K_N \mapsto \mathbf{K}_N = \frac{v_0}{2} \mathbf{T}^T \begin{pmatrix} \frac{\partial^2 t}{\partial m_x^2} & \frac{\partial^2 t}{\partial m_x \partial m_y} \\ \frac{\partial^2 t}{\partial m_y \partial m_x} & \frac{\partial^2 t}{\partial m_y^2} \end{pmatrix} \mathbf{T}$$

From scalar horizontal slowness to horizontal slowness vector:

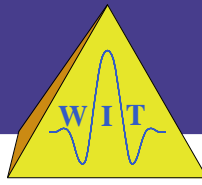
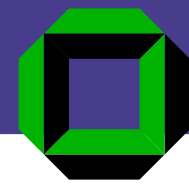
$$p_x \mapsto \begin{pmatrix} p_x \\ p_y \end{pmatrix} = \frac{1}{2} \begin{pmatrix} \frac{\partial t}{\partial m_x} \\ \frac{\partial t}{\partial m_y} \end{pmatrix}$$

Finite-offset vs. zero-offset case



Zero-offset case:

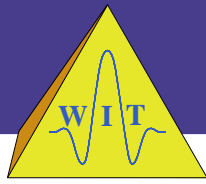
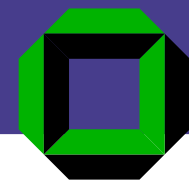
Finite-offset vs. zero-offset case



Zero-offset case:

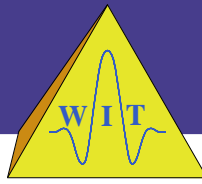
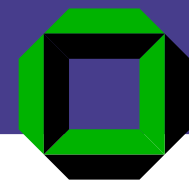
- NIP and normal wavefronts from one-way experiments (exploding reflector and exploding reflection point)

Finite-offset vs. zero-offset case



Zero-offset case:

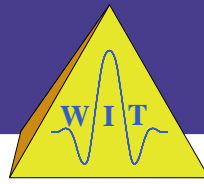
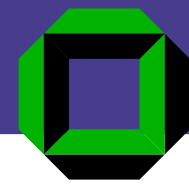
- NIP and normal wavefronts from one-way experiments (exploding reflector and exploding reflection point)
- vivid relation to reflector properties



Zero-offset case:

- NIP and normal wavefronts from one-way experiments (exploding reflector and exploding reflection point)
- vivid relation to reflector properties
- approximate diffraction traveltimes readily available

Finite-offset vs. zero-offset case

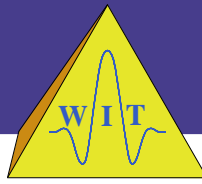
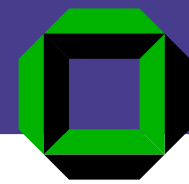


Zero-offset case:

- NIP and normal wavefronts from one-way experiments (exploding reflector and exploding reflection point)
- vivid relation to reflector properties
- approximate diffraction traveltimes readily available

Finite-offset case:

Finite-offset vs. zero-offset case



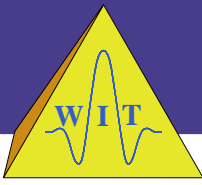
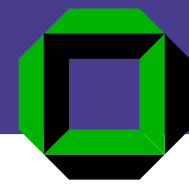
Zero-offset case:

- NIP and normal wavefronts from one-way experiments (exploding reflector and exploding reflection point)
- vivid relation to reflector properties
- approximate diffraction traveltimes readily available

Finite-offset case:

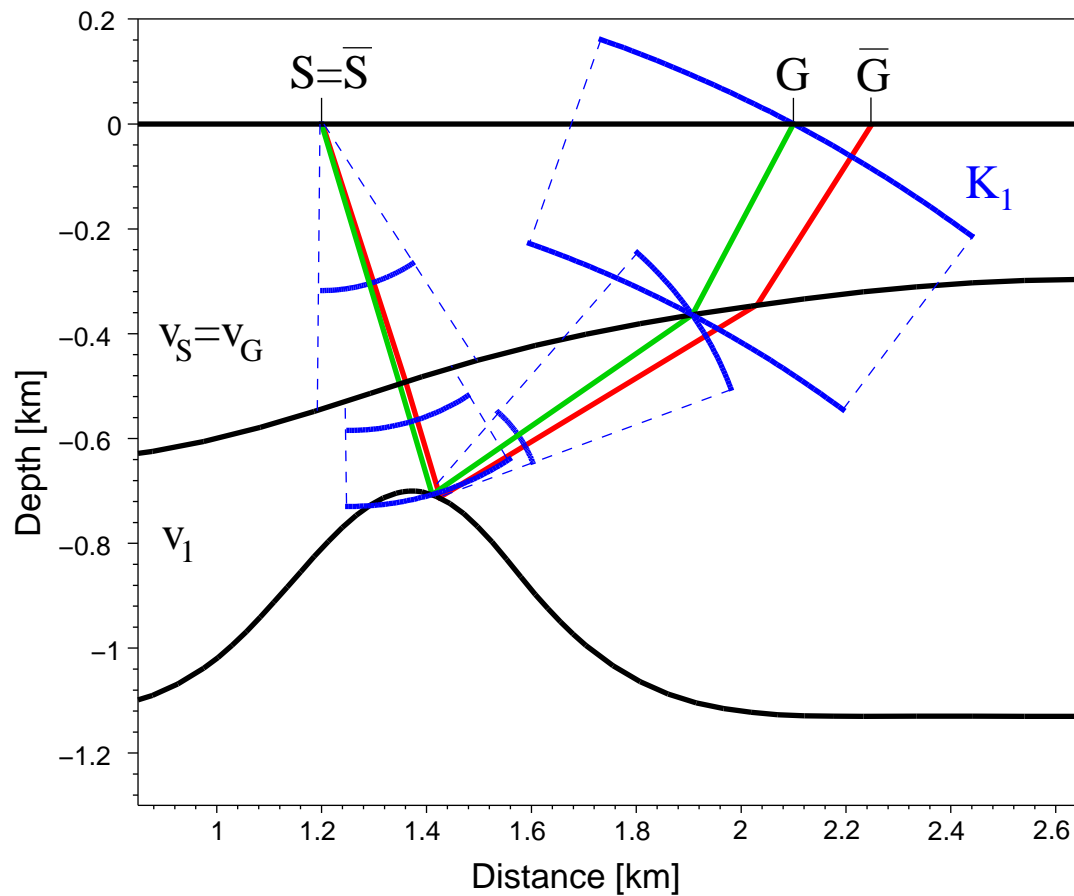
- more complicated hypothetical experiments required, including reflection

Finite-offset vs. zero-offset case

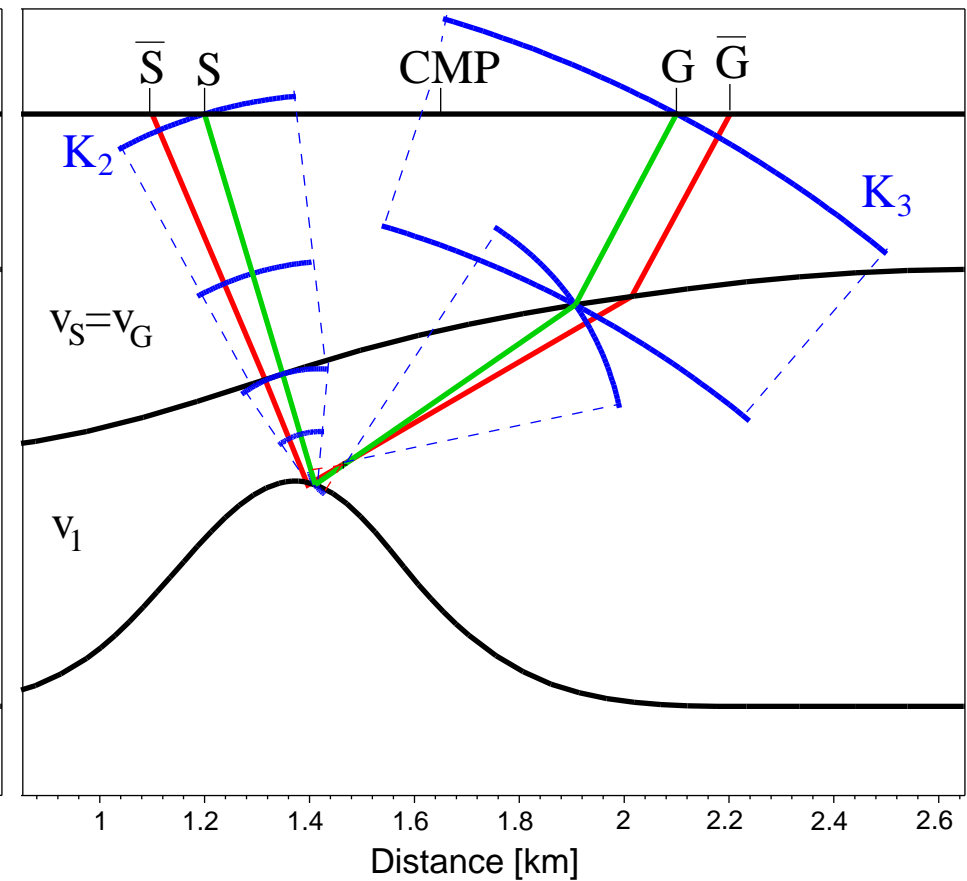


Hypothetical experiments in the finite-offset case

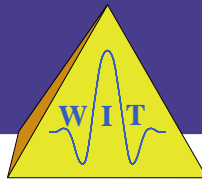
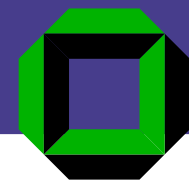
Common-shot experiment



Common-midpoint experiment



Finite-offset vs. zero-offset case



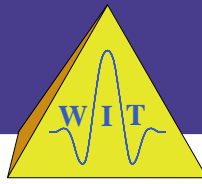
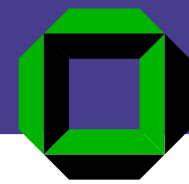
Zero-offset case:

- NIP and normal wavefronts from one-way experiments (exploding reflector and reflection point)
- vivid relation to reflector properties
- approximate diffraction traveltimes readily available

Finite-offset case:

- more complicated hypothetical experiments required, including reflection

Finite-offset vs. zero-offset case



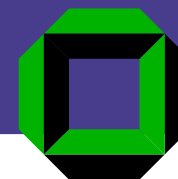
Zero-offset case:

- NIP and normal wavefronts from one-way experiments (exploding reflector and reflection point)
- vivid relation to reflector properties
- approximate diffraction traveltimes readily available

Finite-offset case:

- more complicated hypothetical experiments required, including reflection
- diffraction traveltimes have to be approximated separately

Finite-offset vs. zero-offset case



Zero-offset case:

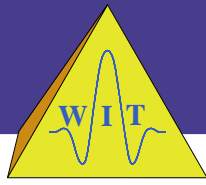
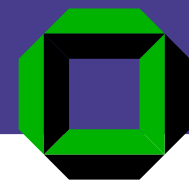
- NIP and normal wavefronts from one-way experiments (exploding reflector and reflection point)
- vivid relation to reflector properties
- approximate diffraction traveltimes readily available

Finite-offset case:

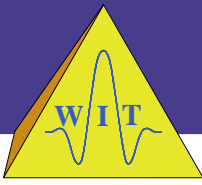
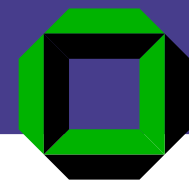
- more complicated hypothetical experiments required, including reflection
- diffraction traveltimes have to be approximated separately

 presentation by Bergler and Hubral in this session 

Applications of attributes

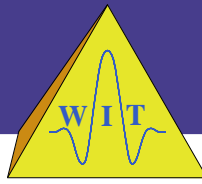
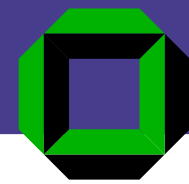


Applications of attributes



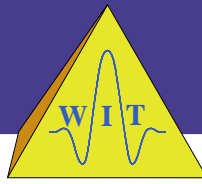
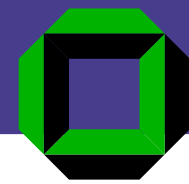
- Construction of interval velocity models based on picked zero-offset traveltimes and attributes with

Applications of attributes



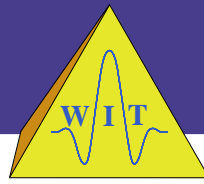
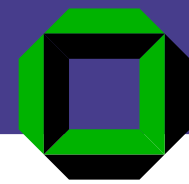
- Construction of interval velocity models based on picked zero-offset traveltimes and attributes with
 - a generalized Dix-type inversion:

Applications of attributes



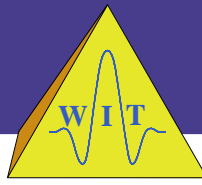
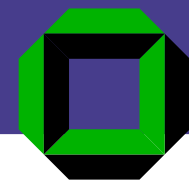
- Construction of interval velocity models based on picked zero-offset traveltimes and attributes with
 - a generalized Dix-type inversion:
 - layer stripping approach

Applications of attributes



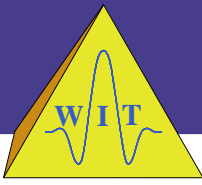
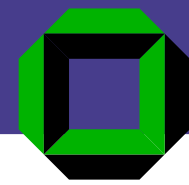
- Construction of interval velocity models based on picked zero-offset traveltimes and attributes with
 - a generalized Dix-type inversion:
 - layer stripping approach
 - downward propagation of NIP wavefronts until
$$R_{NIP} = 0 \wedge t_0 = 0$$

Applications of attributes



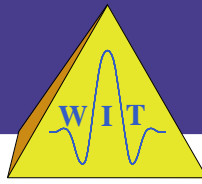
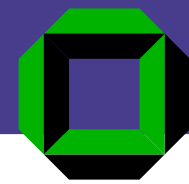
- Construction of interval velocity models based on picked zero-offset traveltimes and attributes with
 - a generalized Dix-type inversion:
 - layer stripping approach
 - downward propagation of NIP wavefronts until
$$R_{NIP} = 0 \wedge t_0 = 0$$
 - a tomographic approach:

Applications of attributes



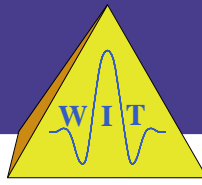
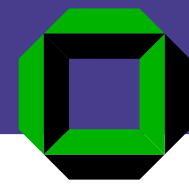
- Construction of interval velocity models based on picked zero-offset traveltimes and attributes with
 - a generalized Dix-type inversion:
 - layer stripping approach
 - downward propagation of NIP wavefronts until
$$R_{NIP} = 0 \wedge t_0 = 0$$
 - a tomographic approach:
 - initial model of interval velocity and reflector segments

Applications of attributes



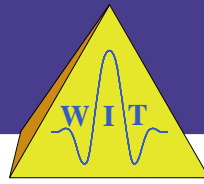
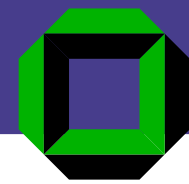
- Construction of interval velocity models based on picked zero-offset traveltimes and attributes with
 - a generalized Dix-type inversion:
 - layer stripping approach
 - downward propagation of NIP wavefronts until
$$R_{NIP} = 0 \wedge t_0 = 0$$
 - a tomographic approach:
 - initial model of interval velocity and reflector segments
 - forward modeling of NIP wavefronts

Applications of attributes

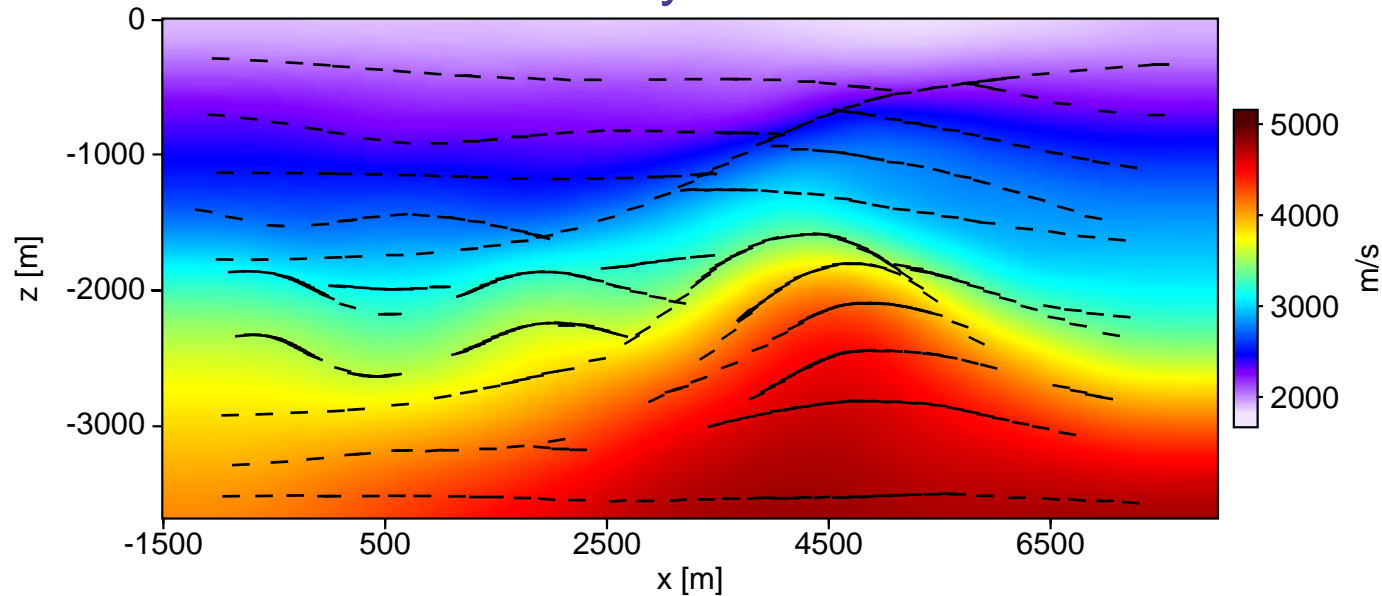


- Construction of interval velocity models based on picked zero-offset traveltimes and attributes with
 - a generalized Dix-type inversion:
 - layer stripping approach
 - downward propagation of NIP wavefronts until
$$R_{NIP} = 0 \wedge t_0 = 0$$
 - a tomographic approach:
 - initial model of interval velocity and reflector segments
 - forward modeling of NIP wavefronts
 - iterative model updates to minimize misfit

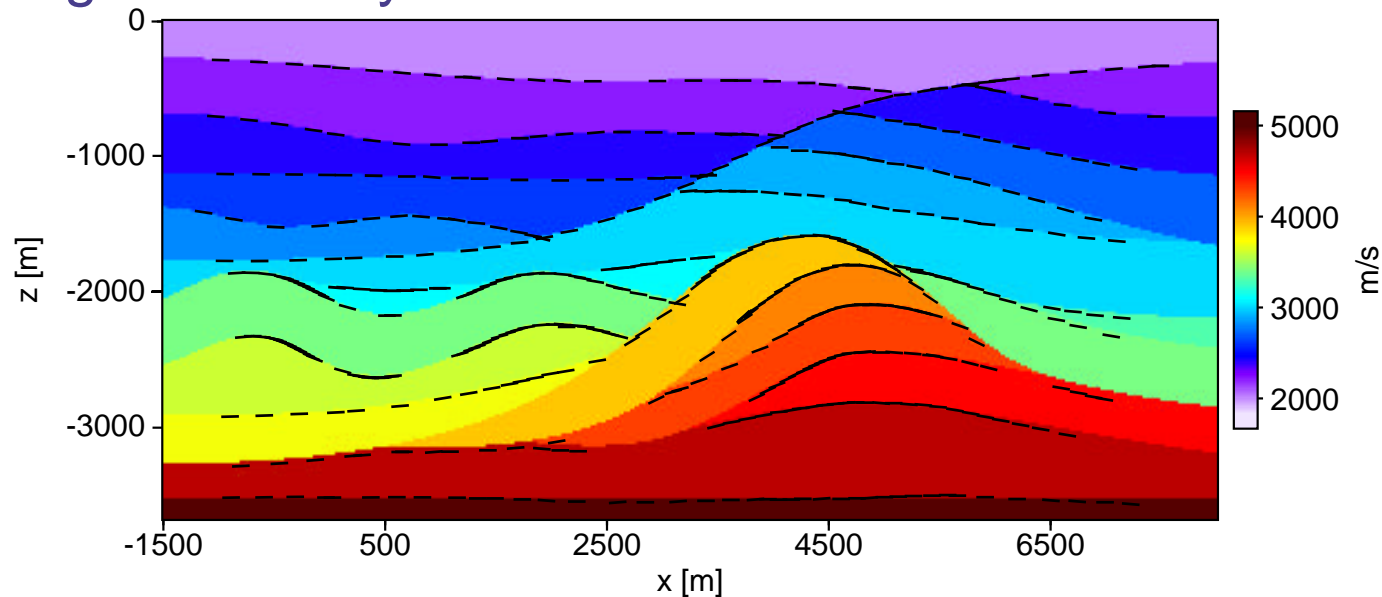
Reconstructed vs. original model



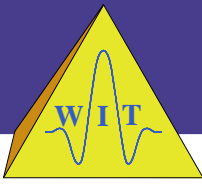
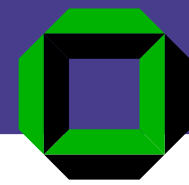
Reconstructed velocity and reflector elements



Original velocity and reconstructed reflector elements

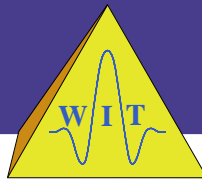
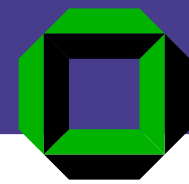


Applications of attributes



- Construction of interval velocity models based on picked zero-offset traveltimes and attributes with
 - a generalized Dix-type inversion:
 - layer stripping approach
 - downward propagation of NIP wavefronts until
$$R_{NIP} = 0 \wedge t_0 = 0$$
 - a tomographic approach:
 - initial model of interval velocity and reflector segments
 - forward modeling of NIP wavefronts
 - iterative model updates to minimize misfit

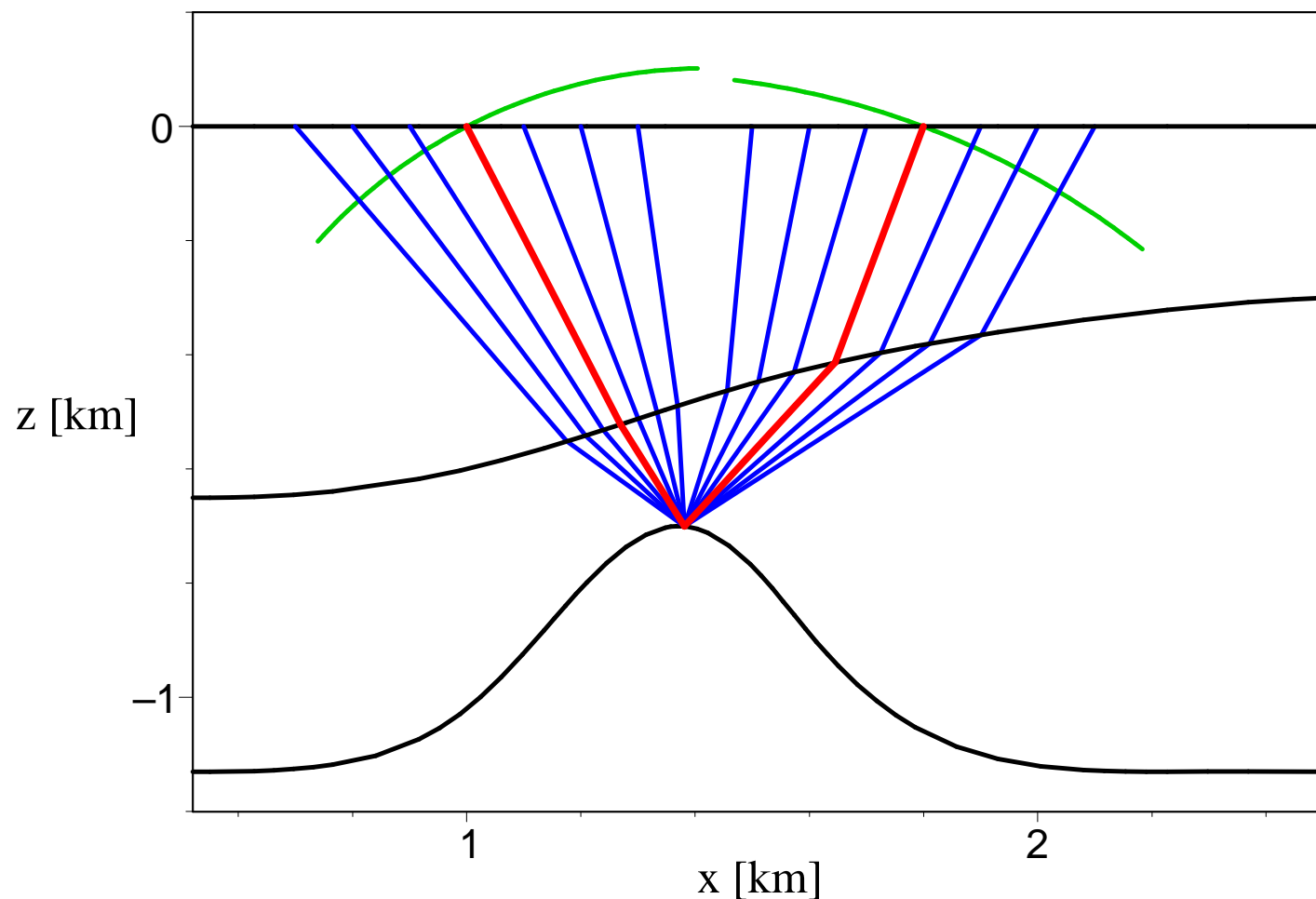
Applications of attributes



- Construction of interval velocity models based on picked zero-offset traveltimes and attributes with
 - a generalized Dix-type inversion:
 - layer stripping approach
 - downward propagation of NIP wavefronts until
$$R_{NIP} = 0 \wedge t_0 = 0$$
 - a tomographic approach:
 - initial model of interval velocity and reflector segments
 - forward modeling of NIP wavefronts
 - iterative model updates to minimize misfit
- 👉 presentation by Duveneck tomorrow 👈



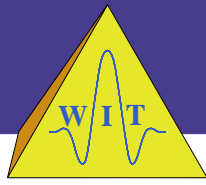
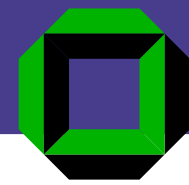
Wavefronts for generalized Stereotomography



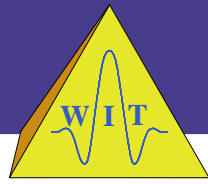
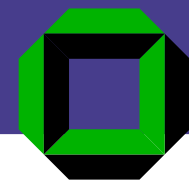
presentation by Bergler and Hubral today



Applications of attributes

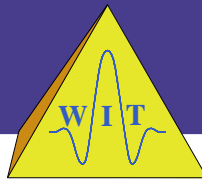
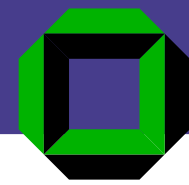


Applications of attributes



Based on approximation of diffraction traveltimes:

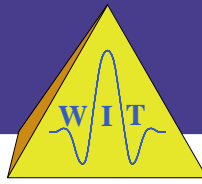
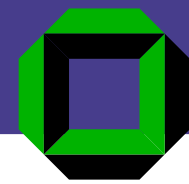
Applications of attributes



Based on approximation of diffraction traveltimes:

- approximation of geometrical spreading factor

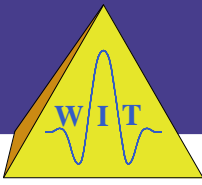
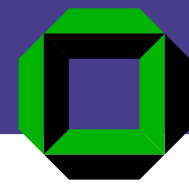
Applications of attributes



Based on approximation of diffraction traveltimes:

- approximation of geometrical spreading factor
- approximation of projected Fresnel zone

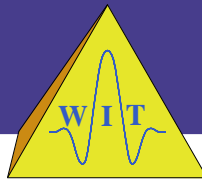
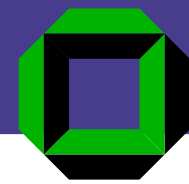
Applications of attributes



Based on approximation of diffraction traveltimes:

- approximation of geometrical spreading factor
- approximation of projected Fresnel zone
- data-driven time migration

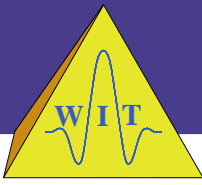
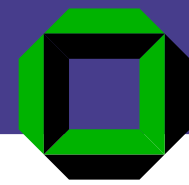
Applications of attributes



Based on approximation of diffraction traveltimes:

- approximation of geometrical spreading factor
- approximation of projected Fresnel zone
- data-driven time migration
- identification of diffraction events

Applications of attributes

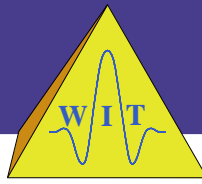
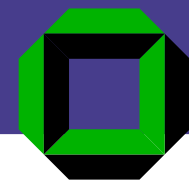


Based on approximation of diffraction traveltimes:

- approximation of geometrical spreading factor
- approximation of projected Fresnel zone
- data-driven time migration
- identification of diffraction events

Extensions based on attribute extrapolation at surface:

Applications of attributes



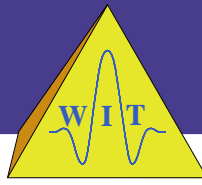
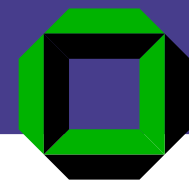
Based on approximation of diffraction traveltimes:

- approximation of geometrical spreading factor
- approximation of projected Fresnel zone
- data-driven time migration
- identification of diffraction events

Extensions based on attribute extrapolation at surface:

- CRS stack with topography

Applications of attributes



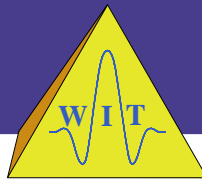
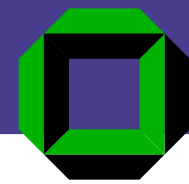
Based on approximation of diffraction traveltimes:

- approximation of geometrical spreading factor
- approximation of projected Fresnel zone
- data-driven time migration
- identification of diffraction events

Extensions based on attribute extrapolation at surface:

- CRS stack with topography
 - direct use of source and receiver elevations

Applications of attributes



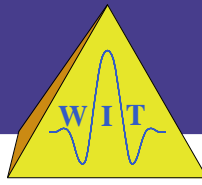
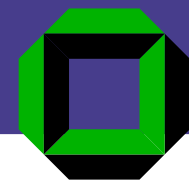
Based on approximation of diffraction traveltimes:

- approximation of geometrical spreading factor
- approximation of projected Fresnel zone
- data-driven time migration
- identification of diffraction events

Extensions based on attribute extrapolation at surface:

- CRS stack with topography
 - direct use of source and receiver elevations
 - wavefield attributes as if recorded on plane surface

Applications of attributes



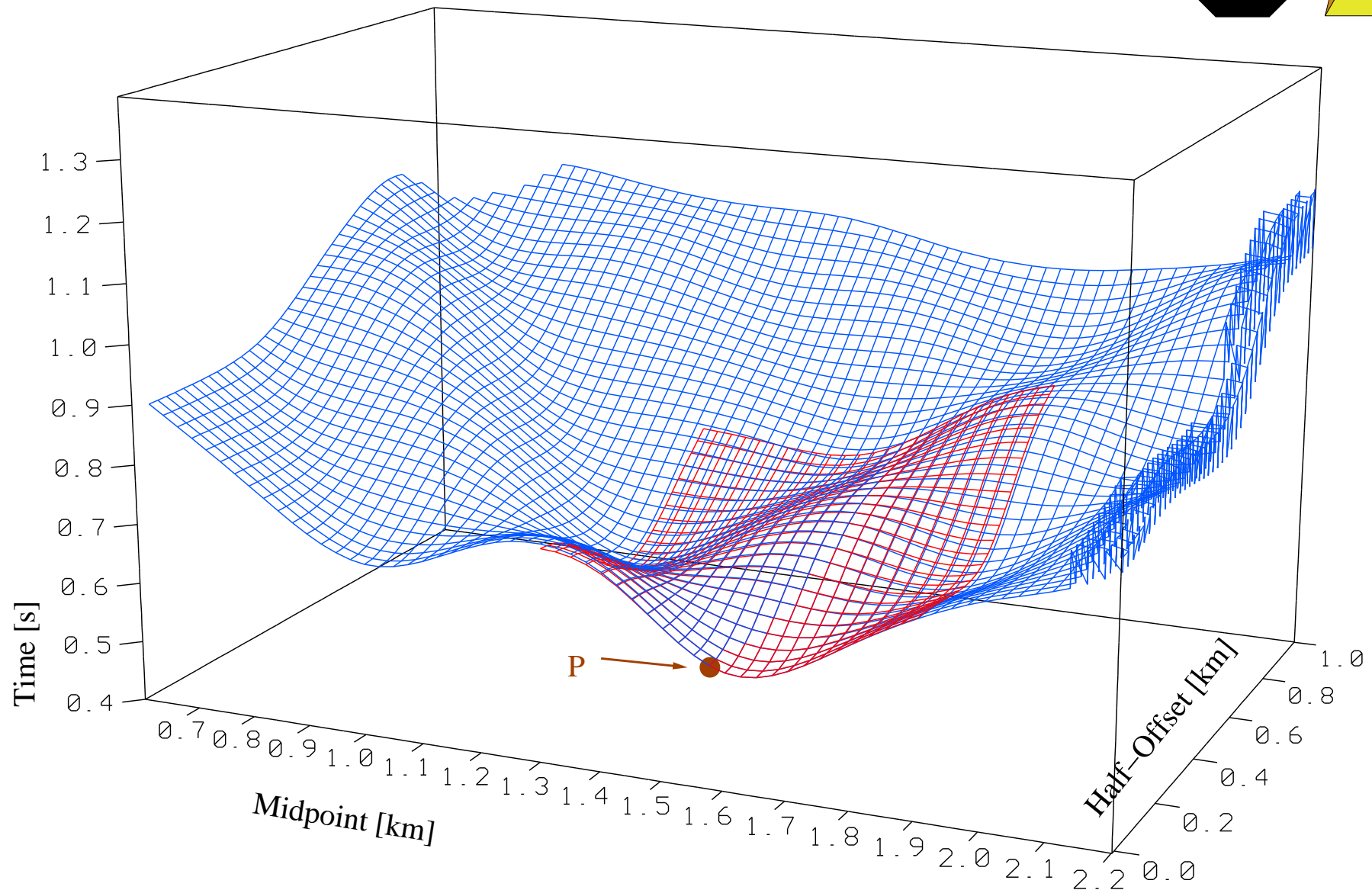
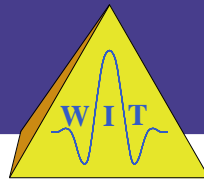
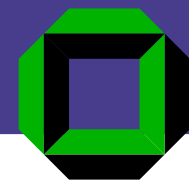
Based on approximation of diffraction traveltimes:

- approximation of geometrical spreading factor
- approximation of projected Fresnel zone
- data-driven time migration
- identification of diffraction events

Extensions based on attribute extrapolation at surface:

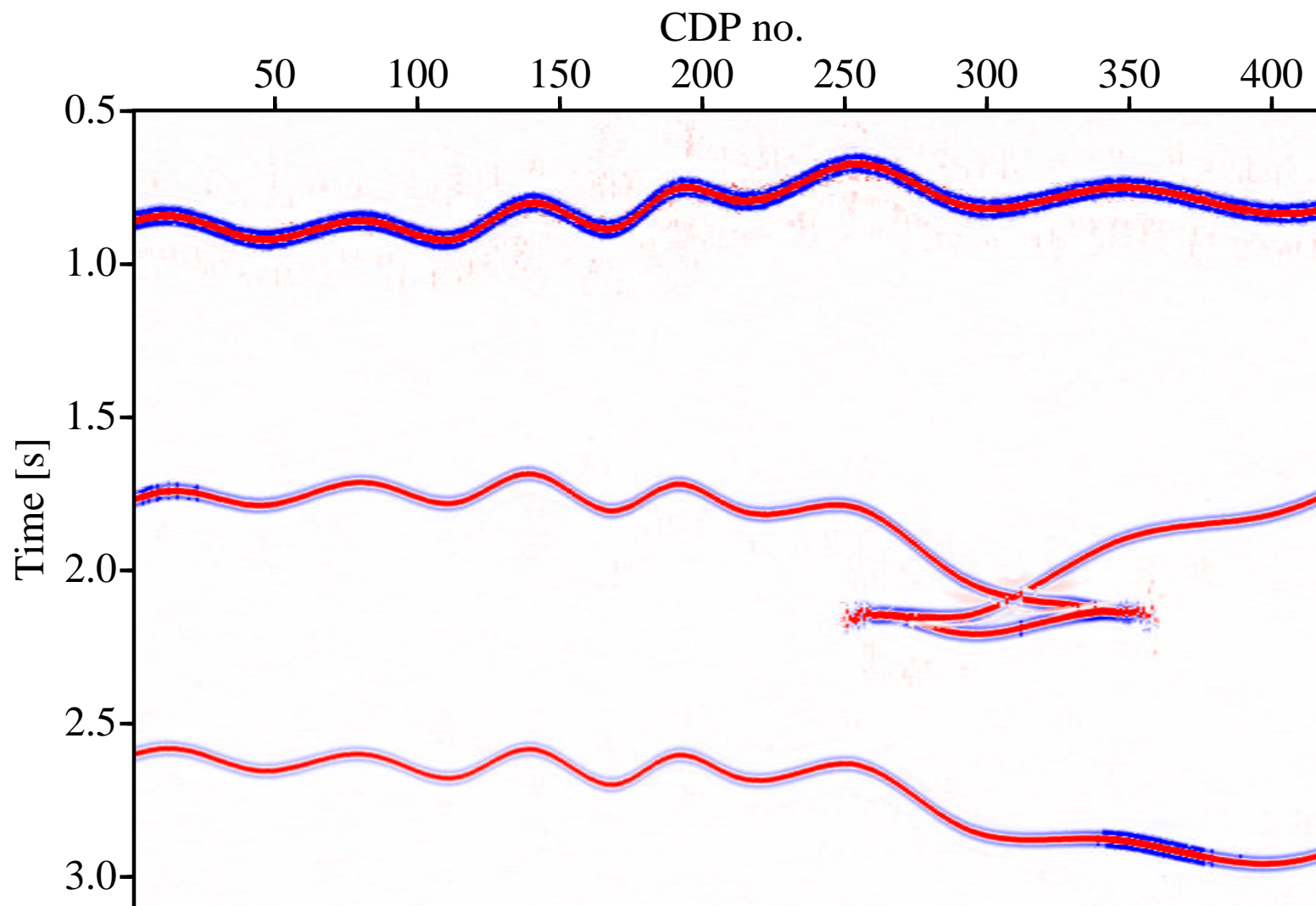
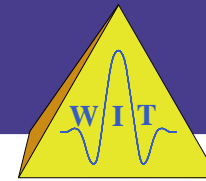
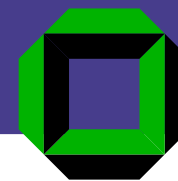
- CRS stack with topography
 - direct use of source and receiver elevations
 - wavefield attributes as if recorded on plane surface
- Redatuming

Applications of attributes



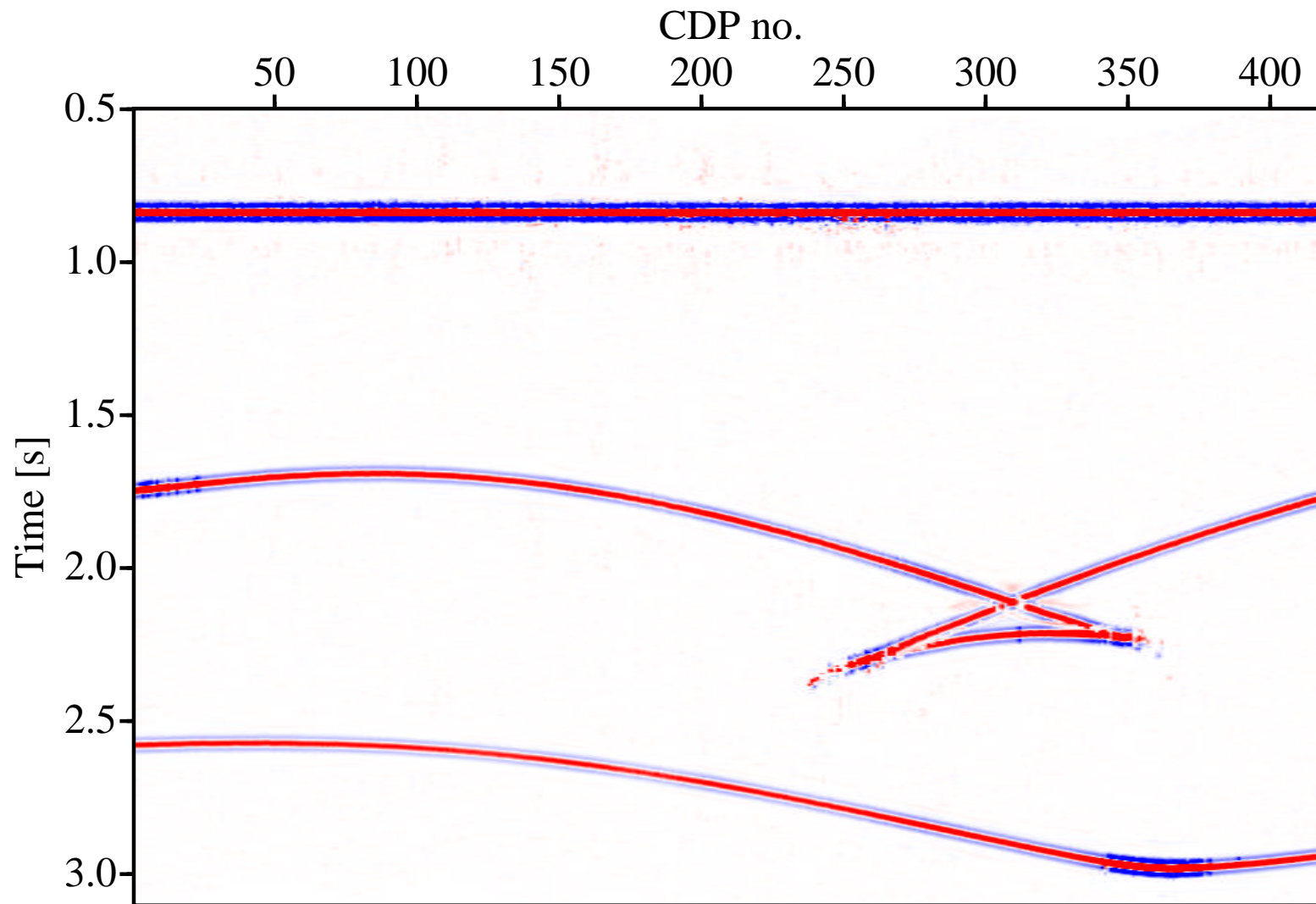
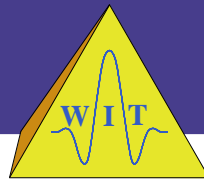
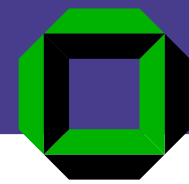
Synthetic example with topography

Applications of attributes



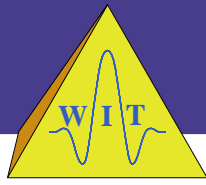
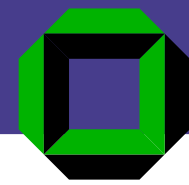
Optimized CRS stack

Applications of attributes



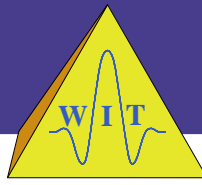
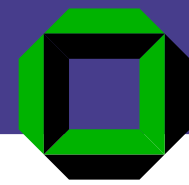
Redatumed CRS stack section

Conclusions



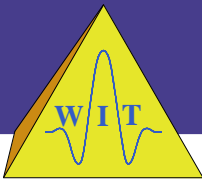
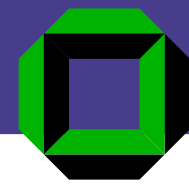
- consequent generalization of classic data-driven approaches

Conclusions



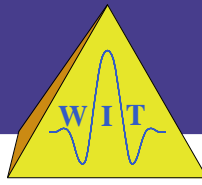
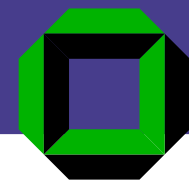
- consequent generalization of classic data-driven approaches
- requires minimum interaction

Conclusions



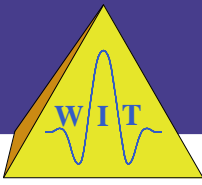
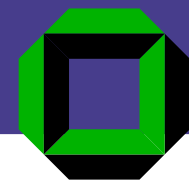
- consequent generalization of classic data-driven approaches
- requires minimum interaction
- provides wavefield attributes for various applications

Conclusions



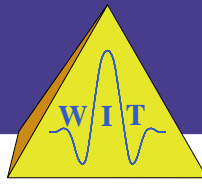
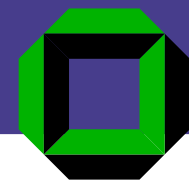
- consequent generalization of classic data-driven approaches
- requires minimum interaction
- provides wavefield attributes for various applications
- allows consistent processing workflow

Conclusions



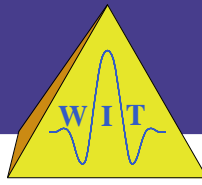
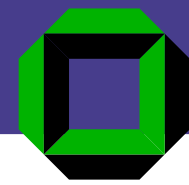
- consequent generalization of classic data-driven approaches
- requires minimum interaction
- provides wavefield attributes for various applications
- allows consistent processing workflow
 - CRS stack

Conclusions



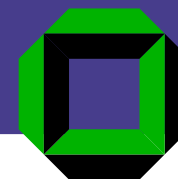
- consequent generalization of classic data-driven approaches
- requires minimum interaction
- provides wavefield attributes for various applications
- allows consistent processing workflow
 - CRS stack
 - attribute-based velocity determination

Conclusions

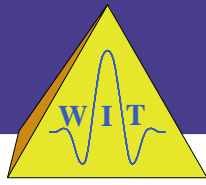
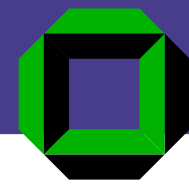


- consequent generalization of classic data-driven approaches
- requires minimum interaction
- provides wavefield attributes for various applications
- allows consistent processing workflow
 - CRS stack
 - attribute-based velocity determination
 - poststack migration of CRS result and/or

Conclusions

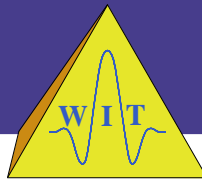
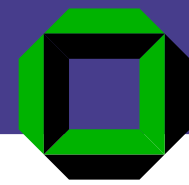


- consequent generalization of classic data-driven approaches
- requires minimum interaction
- provides wavefield attributes for various applications
- allows consistent processing workflow
 - CRS stack
 - attribute-based velocity determination
 - poststack migration of CRS result and/or
 - prestack migration based on inversion result

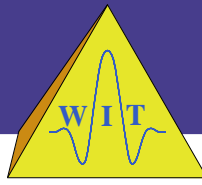
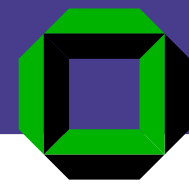


- implementation of 3-D inversion
(in progress)

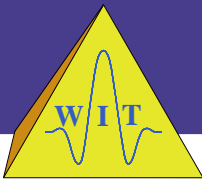
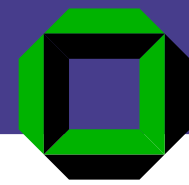
Outlook



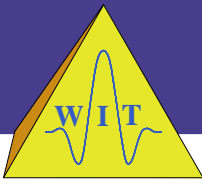
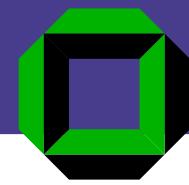
- implementation of 3-D inversion
(in progress)
- implementation of finite-offset inversion
(in progress)



- implementation of 3-D inversion
(in progress)
- implementation of finite-offset inversion
(in progress)
- application of complete workflow to real data



- implementation of 3-D inversion
(in progress)
- implementation of finite-offset inversion
(in progress)
- application of complete workflow to real data
- use of approximated projected Fresnel zone for
limited aperture migration



- implementation of 3-D inversion
(in progress)
- implementation of finite-offset inversion
(in progress)
- application of complete workflow to real data
- use of approximated projected Fresnel zone for
limited aperture migration
- further applications

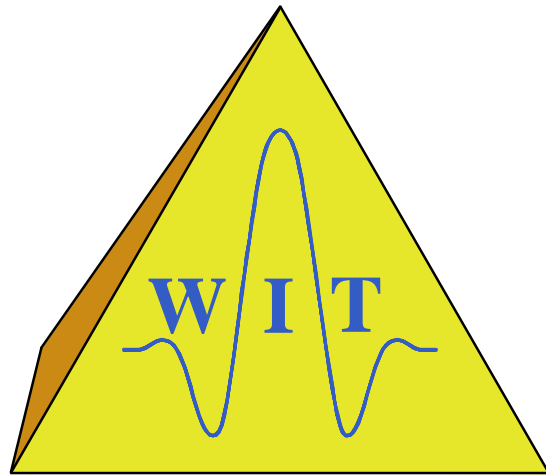
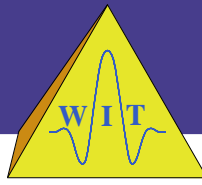
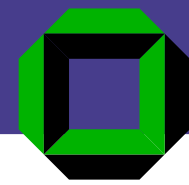


- implementation of 3-D inversion
(in progress)
- implementation of finite-offset inversion
(in progress)
- application of complete workflow to real data
- use of approximated projected Fresnel zone for
limited aperture migration
- further applications
 - CRS-based residual static corrections



- implementation of 3-D inversion
(in progress)
- implementation of finite-offset inversion
(in progress)
- application of complete workflow to real data
- use of approximated projected Fresnel zone for
limited aperture migration
- further applications
 - CRS-based residual static corrections
 - data regularization

Acknowledgments



This work was supported by the sponsors of the *Wave Inversion Technology Consortium*.